AFGL-TR-82-0223

SIO Ref. 83-10

AD-A 133 979

IMPLICATIONS OF THE EQUATION OF TRANSFER WITHIN THE VISIBLE AND INFRARED SPECTRUM

Jacqueline I. Gordon

Scientific Report No. 1
August 1982

Contract No. F19628-82-C-0060
Project No. 7670
Task No. 7670-14
Work Unit No. 7670-14-02

Contract Monitor, Major John D. Mill, USAF
Optical Physics Division

Prepared for
Air Force Geophysics Laboratory, Air Force Systems Command
United States Air Force, Hanscom AFB, Massachusetts 01731

UNIVERSITY OF CALIFORNIA SAN DIEGO

SCRIPPS INSTITUTION OF OCEANOGRAPHY

VISIBILITY LABORATORY La Jolla, California 92093

UNCLASSIFIED

SECURITY CLASSIFICATION OF THIS PAGE (When Data Entered)

REPORT DOCUMENTATION PAGE		READ INSTRUCTIONS BEFORE COMPLETING FORM
1. REPORT NUMBER AFGL-TR-82-0223	2. GOVT ACCESSION NO.	3. RECIPIENT'S CATALOG NUMBER
4. TITLE (and Subtitle) IMPLICATIONS OF THE EQUATION OF TRANSFER WITHIN THE VISIBLE AND INFRARED SPECTRUM		5. TYPE OF REPORT & PERIOD COVERED Scientific - Interim Scientific Report No. 1 6. PERFORMING ORG. REPORT NUMBER SIO Ref. 83-10
7. AUTHOR(s) Jacqueline I. Gordon		8. CONTRACT OR GRANT NUMBER(s) F19628-82-C-0060
9. PERFORMING ORGANIZATION NAME AND ADDRESS University of California, San Diego Visibility Laboratory La Jolla, California 92093		10. PROGRAM ELEMENT, PROJECT, TASK AREA & WORK UNIT NUMBERS 62101F 7670-14-02
11. CONTROLLING OFFICE NAME AND ADDRESS Air Force Geophysics Laboratory Hanscom AFB, Massachusetts 01731 Contract Monitor: Major John D. Mill/OPA		12. REPORT DATE August 1982 13. NUMBER OF PAGES 55
14. MONITORING AGENCY NAME & ADDRESS(if different from Controlling Office)		15. SECURITY CLASS. (of this report) UNCLASSIFIED 15a. DECLASSIFICATION/DOWNGRADING SCHEDULE

16. DISTRIBUTION STATEMENT (of this Report)

Approved for public release; distribution unlimited.

17. DISTRIBUTION STATEMENT (of the abstract entered in Block 20, if different from Report)

18. SUPPLEMENTARY NOTES

19. KEY WORDS (Continue on reverse side if necessary and identify by block number)

Equation of Transfer
Solar Almucantar
Volume Scattering Function

20. ABSTRACT (Continue on reverse side if necessary and identify by block number)

The equation of transfer for radiance, irradiance and scalar irradiance is fully defined and integrated for a scattering, absorbing and emitting medium. Some of the special characteristics of the solar almucantar are delineated as well as methods presented for using the solar almucantar sky radiance to obtain radiance transmittance, test optical stability, and/or test for spurious sun reflectance in the sky radiance photometer. Measurements made with the Visibility Laboratory integrating nephelometer are reviewed and compared to the Barteneva (1960) catalog of photopic volume scattering functions. An average volume scattering function is derived

DD FORM 1 JAN 73 1473 EDITION OF 1 NOV 65 IS OBSOLETE
S/N 0102-014-6601

UNCLASSIFIED

SECURITY CLASSIFICATION OF THIS PAGE (When Data Entered)

20. ABSTRACT continued:

and methods developed for obtaining: 1) the single scattering albedo from horizon sky radiance, 2) the scattering transmittance from sky radiance ratios, and 3) the aerosol optical thickness from solar almucantar radiances.

AFGL-TR-82-0223 SIO Ref. 83-10

IMPLICATIONS OF THE EQUATION OF TRANSFER WITHIN THE VISIBLE AND INFRARED SPECTRUM

Jacqueline I. Gordon

Visibility Laboratory
University of California, San Diego
Scripps Institution of Oceanography
La Jolla, California 92093

Approved:

R. W. Austin

Roswell W. Austin, Director
Visibility Laboratory

Approved:

William A. Nierenberg

William A. Nierenberg, Director
Scripps Institution of Oceanography

CONTRACT NO. F19628-82-C-0060
Project No. 7670
Task No. 7670-14
Work Unit No. 7670-14-02

Scientific Report No. 1
August 1982

Contract Monitor
Major John D. Mill, Atmospheric Optics Branch, Optical Physics Division

Prepared for

AIR FORCE GEOPHYSICS LABORATORY
AIR FORCE SYSTEMS COMMAND
UNITED STATES AIR FORCE
HANSCOM AFB, MASSACHUSETTS 01731

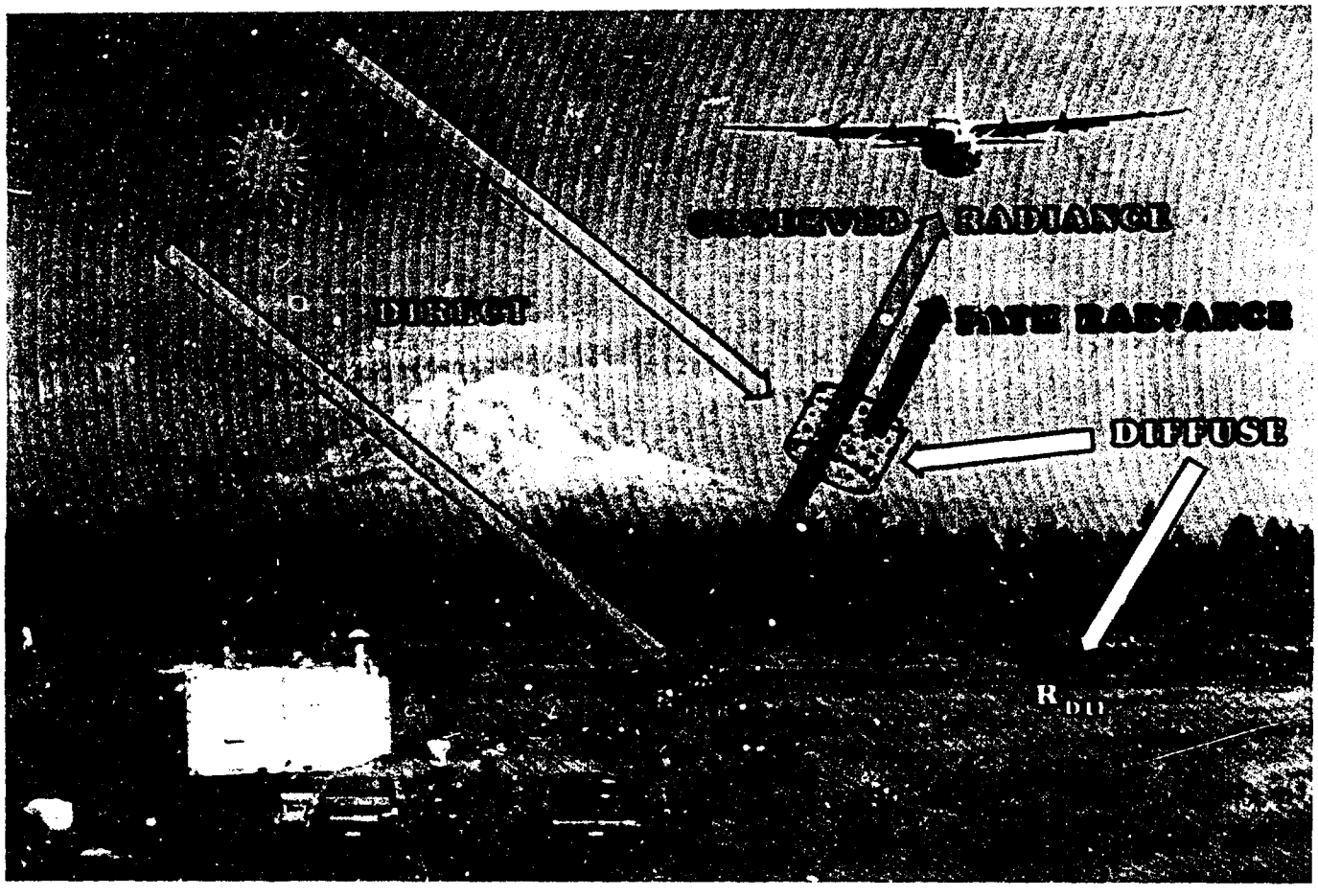

Frontispiece

The composite scene above pictorially illustrates many of the radiometric relationships from which the implications discussed in this report and derived. The photographic portion illustrates a joint airborne/groundbased experimental measurements program conducted in the vicinity of Mt. Ranier, Washington by the Visibility Laboratory of the University of California, San Diego, in cooperation with and under the sponsorship of the Air Force Geophysics Laboratory. The cartoon overlay illustrates the influence of the direct and diffuse light fields upon surface targets and the atmospheric path between the surface and the airborne observer. Within the visible spectrum, these atmospheric processes are primarily scattering in nature. Whereas, within the infrared regions, the processes must be expanded to include the effects of absorption and emission. A discussion of these combined effects and their interrelationships is the primary content of this report.

SUMMARY

This report is a part of the Visibility Laboratory's Project OPAQUE effort and was prepared under AFGL Contract F19628-82-C-0060. It describes a review of the theoretical constructs for a radiation medium which scatters, absorbs and emits radiation with special emphasis on applications to the visible and the infrared.

The equation of transfer for radiance, irradiance and scalar irradiance is fully defined and then integrated. If the 4π radiance distribution is measured at several altitudes, the radiance arrays can be tested for consistency and, if consistent, a measure of absorption obtained.

Some of the special characteristics of the solar almucantar are delineated. Methods are presented for using the solar almucantar sky radiance to obtain radiance transmittance, test optical stability, and test for spurious sun reflectance in the sky radiance photometer.

Measurements made with the Visibility Laboratory integrating nephelometer are reviewed and compared to the Barteneva (1960) catalog of photopic volume scattering functions. An average volume scattering function is derived and methods developed for obtaining the single scattering albedo from horizon sky radiance, for obtaining the scattering transmittance from sky radiance ratios, and for obtaining the aerosol optical thickness from solar almucantar radiances.

TABLE OF CONTENTS

LIST OF TABLES AND ILLUSTRATIONS

IMPLICATIONS OF THE EQUATION OF TRANSFER WITHIN THE VISIBLE AND INFRARED SPECTRUM

Jacqueline I. Gordon

1. INTRODUCTION

In the increasingly sophisticated world of electro-optical detection, search, and guidance, the requirement for establishing and predicting atmospheric influences on system performance continues to be a primary operational necessity. It is in support of this requirement that the Visibility Laboratory in cooperation with, and under the sponsorship of the Air Force Geophysics Laboratory has maintained an extensive program of airborne optical and meteorological measurements. In recent years this program has been conducted as an independent but cooperative effort (Johnson *et al.* (1979)) in conjunction with the NATO program OPAQUE (Optical Atmospheric Quantities in Europe), Fenn (1978). During the two year interval spanning the years 1977 and 1978, over 80 missions were flown documenting the vertical structure of the visible spectrum total volume scattering coefficient in the lower troposphere as well as the 4π radiance distribution of the ambient light field at several altitudes. Since a thorough awareness of the vertical structure of volume scattering coefficient is essential to the prediction of atmospheric influences on contrast transmittance through this regime, these data have been presented in a series of technical reports, the two most representative of which are entitled "Airborne Measurements of Atmospheric Volume Scattering Coefficients in Northern Europe, Summer 1978," Johnson and Gordon (1980), and "An Analysis of Natural Variations in European Sky and Terrain Radiance Measurements", Johnson and Hering (1981b).

The optimum use of the experimental data presented in reports such as those referenced above is surely to establish the baseline assessment of those optical characteristics most influencing slant path contrast transmittance, and to develop from these assessments realistic predictive models. An initial effort in this model development, using both surface and profile data from the OPAQUE program is discussed in Johnson *et al.* (1979), and the further application of these data to contrast transmittance modelling is illustrated by Hering (1981a).

In order to extend the methodologies developed for visible spectrum modelling into the infrared, it seems appropriate to review the theoretical constructs for a radiation medium which scatters, absorbs and emits radiation. These constructs are being used to evaluate the data from the atmospheric optical measurement program and develop models. In addition we will review a few of the data sets which have specific modeling implications.

The following section will deal with the basic monochromatic equation of transfer as it relates to radiance, irradiance and scalar irradiance. The concepts will be fully defined and related where possible to the theoretical work of Duntley *et al.* (1957), Preisendorfer (1976) and Chandrasekhar (1960). A table of notational equivalencies for the Chandrasekhar (1960) notation and the Visibility Laboratory notation is given in Appendix B.

The third section will delineate some of the special features of the solar almucantar.

The fourth section will review the measurements made with the Visibility Laboratory integrating nephelometer. These data will be compared to the Barteneva (1960) catalog of photopic volume scattering functions and an average volume scattering function derived. Some of the implications of the average volume scattering function will then be explored.

2. EQUATION OF TRANSFER

2.1 Radiance

The basic equations developed herein are monochromatic. Applicability to broadband sensors will be discussed where appropriate.

The most basic equation in radiation theory is the equation of transfer (Eq. 10 Duntley *et al.* (1957), Eq. (3) Sec. 3.15 Preisendorfer (1976), and Eq. (46) Chandrasekhar (1960))

$$dL(z,\theta,\phi)/dr = -\alpha(z)\, L(z,\theta,\phi) + L_*(z,\theta,\phi). \qquad (2.1)$$

This equation relates the incremental change in radiance $dL(z,\theta,\phi)$ at altitude z in direction zenith angle θ and azimuth ϕ over the incremental path length dr to the attenuation coefficient $\alpha(z)$, the radiance $L(z,\theta,\phi)$ and the path function $L_*(z,\theta,\phi)$. The first term is the loss term and the second is the gain term.

The attenuation or extinction coefficient $\alpha(z)$ is equivalent to the Chandrasekhar (1960) mass attenuation coefficient k times the density ρ. The attenuation coefficient is the sum of the total scattering coefficient $s(z)$ plus the absorption coefficient $a(z)$

$$\alpha(z) = s(z) + a(z). \qquad (2.2)$$

The path function $L_*(z,\theta,\phi)$ is equivalent to the Chandrasekhar (1960) mass emission coefficient j times the density ρ. The path function is the sum of a scattered component and an emitted component which is related to the absorption

$$L_*(z,\theta,\phi) = L_{*_S}(z,\theta,\phi) + L_{*_a}(z). \qquad (2.3)$$

The emitted component due to absorption is isotropic and hence is shown without direction modifiers.

Scattering

The scattering coefficient has two components. Rayleigh or molecular scattering ${}_RS$ is highly wavelength dependent being proportional to the inverse fourth power of the wavelength λ^{-4}. Mie scattering ${}_MS$ is less wavelength dependent. Both tend to be smooth continuous functions with wavelength.

The path function due to scattering is the integral of the incoming radiance $L(z,\theta',\phi')$ in all 4π directions (including the sun where appropriate) times the volume scattering function $\sigma(z,\beta')$

$$L_{*_s}(z,\theta,\phi) = \int_{4\pi} L(z,\theta',\phi')\,\sigma(z,\beta')\,d\Omega. \qquad (2.4)$$

The scattering angle β' is equivalent to the Chandrasekhar (1960) angle Θ. It is a function of the incoming radiance direction angles θ',ϕ' and the sensor direction angles θ,ϕ as follows

$$\cos\beta' = \sin\theta \sin\theta' \cos(\phi'-\phi) + \cos\theta \cos\theta'. \qquad (2.5)$$

The integral of the volume scattering function over 4π is the total scattering coefficient

$$s(z) = \int_{4\pi} \sigma(z,\beta)\,d\Omega. \qquad (2.6)$$

The volume scattering function is equivalent to the Chandrasekhar (1960) phase function $p(\cos\Theta)$ times the attenuation coefficient α divided by 4π.

Absorption and Emission

Atoms and molecules in the gas phase absorb and emit in line and band spectra. The atomic spectra are line spectra and tend to be at the shorter wavelengths. The band spectra are molecular and tend to be at the longer wavelengths. The continua are essentially part of the band spectra, weak but broad spectrally.

Molecules in the liquid or solid phase cannot emit line or band spectra but can only emit in a continuous spectrum, the distribution of which is determined by the ambient temperature, in other words like a black or grey body (incomplete radiator). This implies that the absorption spectrum for liquids and solids is also continuous spectrally.

An aerosol is defined as a mixture of gas and small solid or liquid particles. Although the solid particulates and water droplets with dissolved particulates absorb and emit like a grey body with a continuous absorption spectrum, the gas or air absorbs and emits in line and band spectra. Thus the aerosol absorbs and emits like a spectral or colored body.

Emission Mechanisms. The principal emission mechanisms above the mesosphere are electroluminescence and chemiluminescence resulting in line and band spectra. These emissions are called airglow. These are important in the visible part of the spectrum at twilight and night but will not be dealt with herein.

The principle emission mechanism in the troposphere and in the atmosphere at or below the mesosphere is temperature radiation which is photon emission caused by atomic or molecular collision. The atmosphere is assumed to be in local thermodynamic equilibrium, hence Kirkhoff's law applies. The path function due to emission is thus [Eq. (38) Chandrasekhar (1960)]

$$L_{*_a}(z) = a(z)\,L(\lambda,T) \qquad (2.7)$$

where $L(\lambda,T)$ is the blackbody radiance at wavelength λ and T is the temperature in degrees Kelvin. The path function due to emittance at and below the mesosphere is highly wavelength dependent and should be dealt with monochromatically.

A black body in thermodynamic equilibrium absorbs and emits as a continuous function of wavelength and temperature according to the classical equation [Wolfe (1978) Table 1.7]

$$L(\lambda,T) = c_1 / [\pi \lambda^5 (e^x - 1)] \qquad (2.8)$$

where

$$c_1 = 2\pi hc^2 = 3.741382E{-}16\ Wm^2 \qquad (2.9)$$

and

$$x = c_2 / (\lambda T). \qquad (2.10)$$

The form 3.74E-16 is an alternate format for 3.74×10^{-16}. This computer form is used throughout this report. The c is the speed of light, h is the Planck constant and

$$c_2 = ch/k = 1.438786E{-}2\ mK \qquad (2.11)$$

where k is the Boltzmann constant. The constants are from Driscoll and Vaughn (1978) Table A.1.

Visible Spectrum. Blackbody radiance and hence exitance (emittance) is negligible in the visible spectrum.

Even at $1\mu m$ at 300°K (27°C or 80°F), $L(1\mu m,300K) = 1.76E{-}7\ W/\Omega m^2$. At shorter wavelengths (all the visible wavelengths) and/or lower temperatures (the normal range of temperature below the mesosphere) the emittance is still less. Hence for the visible spectrum Eq. (2.3) becomes

$$L_*(z,\theta,\phi) = L_{*_s}(z,\theta,\phi)\ . \qquad (2.12)$$

Equilibrium Radiance

The equilibrium radiance is defined as the radiance when the incremental change in radiance over the incremental path length dL/dr equals zero, therefore from Eq. (2.1) (Eq. (11) Duntley *et al.* (1957))

$$0 = L_*(z,\theta,\phi) - \alpha(z)\ L_q(z,\theta,\phi) \qquad (2.13)$$

or (Eq. (40) Chandrasekhar(1960))

$$L_q(z,\theta,\phi) = L_*(z,\theta,\phi)\ /\alpha(z)\ . \qquad (2.14)$$

Thus the equilibrium radiance is equal to the Chandrasekhar (1960) source function $\mathcal{J}$.

No Absorption. In a medium or at wavelengths with no absorption, the attenuation coefficient would equal the scattering coefficient and the equilibrium radiance would be equal to

$$L_q(z,\theta,\phi) = L_{*_s}(z,\theta,\phi)/s(z)\ . \qquad (2.15)$$

Scattering Negligible. When scattering is negligible, such as at longer wavelengths in the infrared, the attenuation is equivalent to the absorption. Substituting Eq. (2.7) into Eq. (2.14) we have

$$L_q(z,\theta,\phi) = L(\lambda,T)\ . \qquad (2.16)$$

Equation of Transfer. An alternate form of the equation of transfer is to divide both sides by the attenuation coefficient and let dr equal $sec\theta\ dz$ [Eq. 63 Chandrasekhar (1960)],

$$\cos\theta\ dL\ (z,\theta,\phi)\ /\ [\alpha(z)\ dz]$$
$$= -L(z,\theta,\phi) + L_q(z,\theta,\phi)\ . \qquad (2.17)$$

The $\cos\theta$ is equal to the Chandrasekhar (1960) function μ and $\alpha(z)\ dz$ is equal to $dt(z)$ the differential of the optical thickness $t(z)$.

Incremental Path Length

For paths of sight at zenith angles θ=0 to 70° and 110 to 180°, the incremental path length is a simple function of the altitude increment and the zenith angle.

$$\Delta r = \Delta z\ sec\theta \qquad (2.18)$$

When used for all paths of sight, this is called the plane parallel atmosphere approximation. The Δr is always non-negative since z is defined as $z_1 - z_2$ (the subscripts increase with the flux direction). See Fig. 2-1.

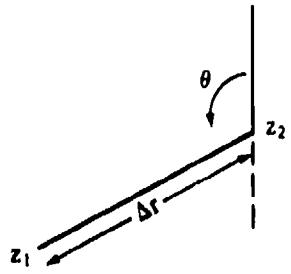

Fig. 2-1. Path length geometry for steeply inclined paths of sight.

For upward-looking paths of sight from 70 to 90 degrees, the Δr for a constant Δz is significantly shorter at altitude than at ground level due to the curvature of the earth. For paths of sight at zenith angles from 90 to 110 degrees, the Δr for a constant Δz is significantly longer at ground level than at altitude also due to the curvature of the earth. Therefore, for these paths of sight, the incremental path length Δr_i is computed from

$$\Delta r_i = \left[\ 1 - \left\{\ n(z)\ (\zeta+z)\sin\theta\ /\ [n(z_i)\ (\zeta+z_i)]\ \right\}^2\ \right]^{-1/2} \Delta z\ . \qquad (2.19)$$

This is the classical equation for computing incremental path length at paths of sight affected by earth curvature and refraction. The $n(z)$ is the refractive index, z is the sensor or observer altitude, ζ is the radius of the earth. Use of the mean earth radius of 6.371229E6 meters results in a maximum error at the equator of -0.1 percent and at the pole of +0.2 percent. See Fig. 2-2 for the relationship of θ and θ'' for the downward (and upward) paths of sight and see Duntley *et al.* (1976) Section 2 for a derivation of Eq. (2.19).

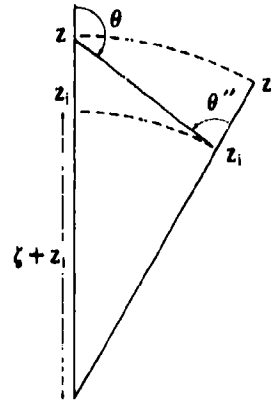

Fig. 2-2. Path length geometry for grazing downward paths of sight in refractive spherical atmospheres. For upward-looking paths of sight the positions z and z_i, and θ and θ'' should be reversed.

2.2 Irradiance

Before deriving the equation of transfer for irradiance, let us first define irradiance and some other terms. The downwelling irradiance $E(z,d)$ is the integral of the radiances from zenith angles 0 to 90 degrees weighted by the cosine of the zenith angle

$$E(z,d) = \int_{2\pi} L(z,\theta',\phi') \cos\theta' \, d\Omega \, . \qquad (2.20)$$

Similarly the upwelling irradiance $E(z,u)$ is computed for angles 90 to 180 degrees by weighting by the cosine of the nadir angle (180-θ) so that the cosine is positive. These are the irradiances on a flat surface oriented to receive the downward and upward radiances respectively.

Scalar Irradiance

A second type of irradiance is the scalar or non-directional irradiance in which the cosine term is not present. The total scalar irradiance $e(z)$ is defined as

$$e(z) = \int_{4\pi} L(z,\theta',\phi') d\Omega \, . \qquad (2.21)$$

The total scalar irradiance is equivalent to the Chandrasekhar (1960) average intensity J times 4π. The scalar irradiance is related to the incoming radiant density w by

$$w = e(z)/c \, , \qquad (2.22)$$

where c is the speed of light.

Scalar Exitance (Emittance)

Exitance (emittance) M is defined with the cosine term similar to the irradiance in Eq. (2.20). Let us define a second type of exitance (emittance) as the scalar or non-directional exitance in which the cosine term is not present. The scalar exitance due to absorption $m(\lambda,T)$ is defined as

$$m(\lambda,T) = L(\lambda,T) \int_{4\pi} d\Omega = 4\pi L(\lambda,T) \, . \qquad (2.23)$$

The scalar exitance is related to the outgoing radiant density $w(\lambda,T)$ by

$$w(\lambda,T) = m(\lambda,T)/c \, . \qquad (2.24)$$

Let us also define another scalar term, scalar exitance per length m_e. This is the unweighted integral over 4π of the path function

$$m_e(z) = \int_{4\pi} L_e(z,\theta,\phi) d\Omega \, . \qquad (2.25)$$

When the path function due to scattering is integrated over 4π it can be expressed as a double integral by substituting in Eq. (2.4)

$$m_{e_s}(z) = \int_{4\pi} \int_{4\pi} L(z,\theta',\phi') \sigma(z,\beta') d\Omega' \, d\Omega \, . \qquad (2.26)$$

Now since the order of integration is unimportant over the double integral, the relationships in Eq. (2.6) and (2.21) can be substituted so that we have the scalar exitance per length due to scattering as

$$m_{e_s}(z) = s(z) \, e(z) \, . \qquad (2.27)$$

Since the path function due to absorption is isotropic the scalar exitance due to absorption is

$$m_{e_a}(z) = a(z) L(\lambda,T) \, 4\pi \, . \qquad (2.28)$$

or

$$m_{e_a}(z) = a(z) m(\lambda,T) \, . \qquad (2.29)$$

Equation of Transfer for Irradiance

The equation of transfer for radiance can be used to obtain an equation of transfer for irradiance by integrating over 4π. First let us rewrite Eq. (2.1) in terms of the separate components of absorption, scattering, and emission and express the incremental path length in terms of Eq. (2.18) thus

$$dL(z,\theta,\phi)\cos\theta/dz = -a(z)L(z,\theta,\phi) - s(z)L(z,\theta,\phi) + L_{e_s}(z,\theta,\phi) + L_{e_a}(z) \, . \qquad (2.30)$$

Now multiplying both sides by $d\Omega$ and expressing both sides as an integral over 4π we get

$$d \int_{4\pi} L(z,\theta,\phi)\cos\theta \, d\Omega \, / \, dz = -a(z) \int_{4\pi} L(z,\theta,\phi) d\Omega - s(z) \int_{4\pi} L(z,\theta,\phi) d\Omega + \int_{4\pi} L_{e_s}(z,\theta,\phi) d\Omega + L_{e_a}(z) \int_{4\pi} d\Omega \, . \qquad (2.31)$$

This can be simplified using Eqs. (2.20), (2.21), (2.27) and (2.29) to become

$$d[E(z,d) - E(z,u)] \, / \, dz = -a(z)e(z) - s(z)e(z) + s(z)e(z) + a(z)m(\lambda,T) \qquad (2.32)$$

This further simplifies to

$$d[E(z,d) - E(z,u)]/dz = -a(z)e(z) + a(z) \, m(\lambda,T) \, . \qquad (2.33)$$

This is the equation for the net irradiance $E(z,d)-E(z,u)$ change with altitude. Let us define $\xi(z)$ as the net irradiance

$$\xi(z) = E(z,d) - E(z,u) . \tag{2.34}$$

Equation (2.33) can now be rewritten as

$$d\xi(z)/dz = a(z)[m(\lambda,T) - e(z)] . \tag{2.35}$$

The net irradiance $\xi(z)$ is equivalent to the Chandrasekhar (1960) net flux πF.

Visible Spectrum. In the visible spectrum where $L(\lambda,T)$ and hence $m(\lambda,T)$ are negligible, Eq. (2.35) can be written as (Eq. 10 Section 1.2 Preisendorfer (1976) since the altitude z is the negative of the depth into the medium)

$$d\xi(z)/dz = -a(z)e(z) . \tag{2.36}$$

The net irradiance either stays constant with altitude indicating no absorption, or decreases as depth into the atmosphere increases. This can be and is being used as a test for the internal consistency of visible spectrum data when measured at a series of altitudes over a period of several hours.

From Eq. (2.36) we also see that in a purely scattering atmosphere there would be no change in net irradiance with altitude.

Equation of Transfer for Scalar Irradiance

An alternate expression is derivable from Eq. (2.30) if we first multiply both sides by $sec\theta$ as well as $d\Omega$ and then integrate. Thus

$$\begin{aligned} &d\int_{4\pi} L(z,\theta,\phi)d\Omega/dz \\ &= -a(z)\int_{4\pi} L(z,\theta,\phi)sec\theta\, d\Omega - s(z)\int_{4\pi} L(z,\theta,\phi)sec\theta\, d\Omega \\ &\quad + \int_{4\pi} L_{e_s}(z,\theta,\phi)sec\theta\, d\Omega + L_{e_a}(z)\int_{4\pi} sec\theta\, d\Omega . \end{aligned} \tag{2.37}$$

Again the middle two terms on the right hand side cancel each other out since the order of integration is not important in a double integral

$$\begin{aligned} &s(z)\int_{4\pi} L(z,\theta,\phi)sec\theta d\Omega \\ &= \int_{4\pi}\int_{4\pi} L(z,\theta',\phi')\sigma(z,\beta')d\Omega sec\theta d\Omega . \end{aligned} \tag{2.38}$$

Also

$$\int_{4\pi} sec\theta d\Omega = 0 , \tag{2.39}$$

since $sec(\pi-\theta) = -sec\theta$. Thus the fourth term also drops out. Now Eq. (2.37) can be written in terms of the change in scalar irradiance with altitude as

$$de(z)/dz = -a(z)\int_{4\pi} L(z,\theta,\phi)sec\theta d\Omega . \tag{2.40}$$

Thus the change in scalar irradiance with altitude is solely a function of absorption and the radiance distribution. The scattering and the path functions due to scattering and absorption do not effect the change in scalar irradiance at any wavelength including the infrared wavelengths. Therefore, when there is no absorption the total scalar irradiance does not change with altitude.

An alternate way of expressing Eq. (2.40) is to separate out the sun term and to express the more diffuse radiances as a radiance difference, sky minus terrain thus

$$\begin{aligned} de(z)/dz &= -a(z)_s e(z)sec\theta_s \\ &\quad - a(z)\int_{2\pi} [L(z,\theta',\phi') - L(z,\pi-\theta',\phi')]sec\theta' d\Omega , \end{aligned} \tag{2.41}$$

where $_se(z)$ is the sun scalar irradiance. Equation (2.41) appears indeterminant because $sec\theta$ goes to infinity at 90 degrees. However, since the radiance difference $L(z,\theta)-L(z,\pi-\theta)$ goes to zero as $sec\theta$ goes to ∞, the equation is not indeterminant and can probably be evaluated with measured radiance distributions.

It is useful at this point to speculate on the relative importance of the two terms in Eq. (2.41). First, we note that at the top of the atmosphere, the sky radiances (θ = 0 to 90 degrees) are zero so that the second term in the equation is positive and the loss due to absorption at all wavelengths is less than due to the solar beam as you begin to descend into the atmosphere.

Now, for additional insight into the two terms for the visible spectrum, let us refer to our existing airborne data on apparent sky and terrain radiances from ground level to 6 kilometers. Figure 2-3 contains two graphs for the AVIZ pseudo-photopic filter (see Appendix A for sensor spectral characteristics), one for high altitude, one for low altitude, of measured sky and terrain radiances for azimuths from the sun ϕ of 0, 90, 180 and 270 degrees. These graphs are typical of terrains with albedos of approximately 0.1. The sky radiances (θ = 0 to 90 degrees) are generally less than the apparent terrain radiances (θ = 90 to 180 degrees) at high altitude and generally greater than the terrain at low altitude. Thus at high altitude the absorption loss or change in $e(z)$ with altitude is less than the absorption due to the solar beam at θ_s, term 1, since the second term is positive. At some intermediate altitude the loss is equivalent to that due to the solar beam since the second term in Eq. (2.41) becomes zero. At low altitude the loss is greater than due to the solar beam since the second term becomes negative.

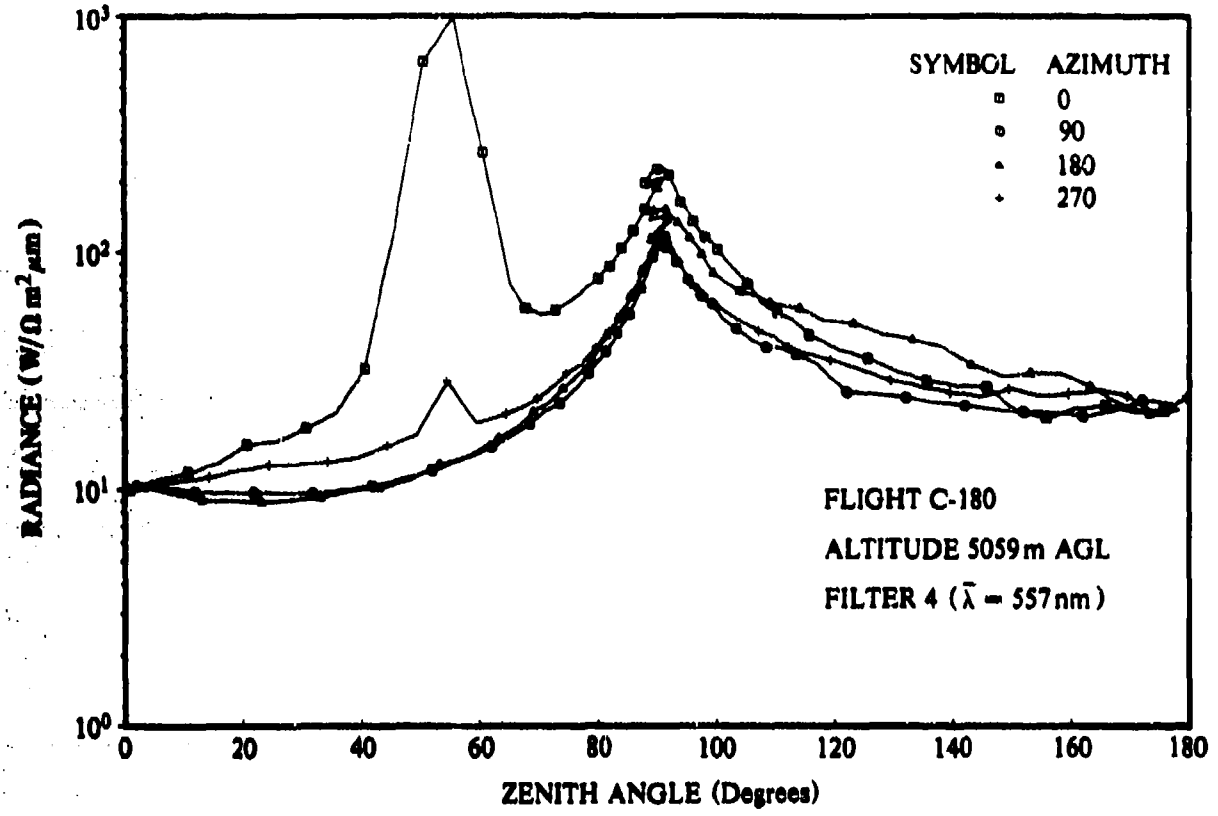

Fig. 2-3a. Sky-terrain radiances for flight C-180, high altitude.

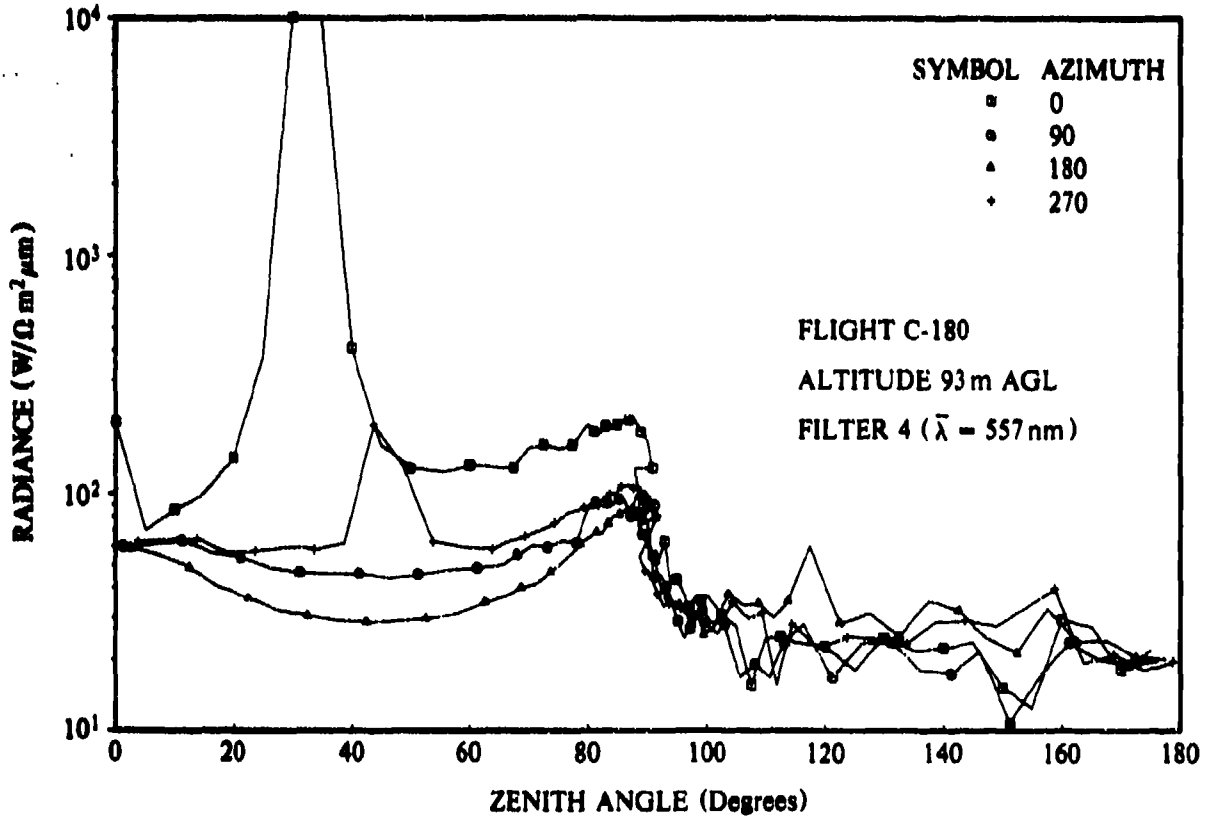

Fig. 2-3b. Sky-terrain radiances for flight C-180, low altitude.

On the same flight, graphs for broad band filters 2 and 3 with mean wavelengths 478 and 664 nm, were similar but the broad band filter 5 mean wavelength 765 nm with an albedo of 0.3, showed sky radiance lower than terrain radiance at low altitude indicating the absorption loss would be less than that indicated by the first term of Eq. (2.41) at all altitudes. This may be typical of measurements for relatively high albedos and high transmittances.

Normalized Functions

Normalized functions have the convenient property of always integrating to one. Thus from Eq. (2.6) we see that the normalized scattering function is $\sigma(z,\beta)/s(z)$ since

$$\int_{4\pi} [\sigma(z,\beta) / s(z)] \, d\Omega = 1 . \qquad (2.42)$$

similarly the normalized scattering path function from Eq. (2.27) is $L_{s_1}(z,\theta,\phi)/(s(z)\epsilon(z))$ since

$$\int_{4\pi} L_{s_1}(z,\theta,\phi) d\Omega \, / \, [s(z)\epsilon(z)] = 1 . \qquad (2.43)$$

Whereas the normalized path function for a medium which emits as well as scatters according to Eqs. (2.27) and (2.29) is

$$\int_{4\pi} L_s(z,\theta,\phi) d\Omega \, / \, [s(z)\epsilon(z) + a(z)m(\lambda,T)] = 1 . \qquad (2.44)$$

Since the equilibrium radiance is the path function divided by the attenuation coefficient (Eq. 2.14) the normalized equilibrium radiance for an emitting and scattering medium is

$$\int_{4\pi} L_q(z,\theta,\phi) d\Omega \; \alpha(z) / [s(z)\epsilon(z) + a(z)m(\lambda,T)] = 1 . \qquad (2.45)$$

The single scattering albedo ω is defined as the ratio of the scattering to the attenuation coefficient

$$\omega(z) = s(z)/\alpha(z) . \qquad (2.46)$$

The normalized equilibrium radiance can be expressed in terms of the single scattering albedo as

$$\int_{4\pi} L_q(z,\theta,\phi) \, d\Omega \, / \, [\omega(z)\epsilon(z) + [1 - \omega(z)] \, m(\lambda,T)] = 1 . \qquad (2.47)$$

Visible Spectrum. For the visible spectrum where emission is negligible the integral of the equilibrium radiance divided by the total scalar irradiance is equal to the single scattering albedo

$$\int_{4\pi} L_q(z,\theta,\phi) \, d\Omega \, / \, \epsilon(z) = \omega(z) . \qquad (2.48)$$

Thus when there is no absorption the equilibrium radiance divided by the total scalar irradiance is the normalized equilibrium radiance,

$$\int_{4\pi} L_q(z,\theta,\phi) \, d\Omega \, / \, \epsilon(z) = 1 . \qquad (2.49)$$

2.3 Integrating the Equation of Transfer

The equation of transfer for radiance Eq. (2.1) when integrated over path length r yields (Eq. 1 Duntley *et al.* (1957), Eq. 1 Section 3.15 Preisendorfer (1976) and Eq. 50 Chandrasekhar (1960))

$$L_r(z,\theta,\phi) = L_0(z_1,\theta,\phi) \; T_r(z,\theta) + L_r^*(z,\theta,\phi) . \qquad (2.50)$$

This equation relates the apparent radiance $L_r(z,\theta,\phi)$ at the sensor altitude z to the inherent radiance $L_o(z_1,\theta,\phi)$ at the target or object altitude z_1 to the radiance transmittance $T_r(z,\theta)$ and the path radiance $L_r^*(z,\theta,\phi)$. The transmittance is expressed as a function of θ but not ϕ since transmittance is not azimuth dependent as long as the attenuation coefficient is assumed to be solely a function of altitude, *i.e.*, the attenuation coefficient is isotropic horizontally.

The radiance transmittance is defined as

$$T_r(z,\theta) = \exp [-t_{\Delta z}(z) sec\theta] . \qquad (2.51)$$

The $t_{\Delta z}(z)$ is the optical thickness in the altitude interval Δz (z_1 to z). The optical thickness is equal to the integral of the attenuation coefficient from z_1 to z

$$t_{\Delta z}(z) = \int_{z_1}^{z} \alpha(z) dz . \qquad (2.52)$$

The path radiance is the integral of the path function times the intervening transmittance (Duntley *et al.* (1957) Eq. (17))

$$L_r^*(z,\theta,\phi) = \int_{z_1}^{z} L_s(z_1,\theta,\phi) \; T_{r_1}(z,\theta) sec\theta dz \qquad (2.53)$$

where r_1 is from z_1 to z.

Horizontal Case

The path radiance for the horizontal case can be expressed as

$$L_r^*(z,90,\phi) = L_s(z,90,\phi) \int_0^r T_{r_1}(z,90) dr \qquad (2.54)$$

since the path function is homogeneous horizontally if the attenuation coefficient is horizontally isotropic. By

multiplying the numerator and denominator by $\alpha(z)$ we can integrate to get

$$L_r^*(z,90,\phi) = L_s(z,90,\phi)[1 - T_r(z,90)] / \alpha(z) \quad (2.55)$$

or from Eq. (2.14)

$$L_r^*(z,90,\phi) = L_q(z,90,\phi)\,[1 - T_r(z,90)]\,. \quad (2.56)$$

This is the standard equation for the horizontal path of sight which holds for a scattering, absorbing and emitting medium which is horizontally homogeneous.

Since the sky radiance is the path radiance from space-to-earth, the horizon sky radiance is

$$L_\infty^*(z,90,\phi) = L_q(z,90,\phi)\,[1 - T_\infty(z,90)]\,. \quad (2.57)$$

The transmittance from space-to-earth at zenith angle θ is a function of the vertical transmittance and the relative optical airmass $m_\infty(z,\theta)/m_\infty(z,0)$. Therefore

$$T_\infty(z,90) = T_\infty(z,0)^{m_\infty(z,90)/m_\infty(z,0)}\,. \quad (2.58)$$

Air Mass

The absolute optical airmass $m_\infty(z,\theta)$ is the mass of an aircolumn of unit cross section which is the integral of the density over the path length from altitude z to ∞

$$m_\infty(z,\theta) = \int_z^\infty \rho(x)\,dr\,. \quad (2.59)$$

The relative optical airmass is the ratio of the airmass at some angle θ to the vertical airmass $m_\infty(z,\theta)/m_\infty(z,0)$. In computations of the optical air mass, the incremental path length Δr_i is computed using Eq. (2.19) which takes into account both the curvature of the earth and refraction. For the computations herein the mean earth radius was used.

The square of the refractive index is expressed as a function of the density ratio by Kasten (1965)

$$[n(z)/n(z_i)]^2 = 1 + 2[n(z) - 1][1 - \rho(z_i)/\rho(z)] \quad (2.60)$$

To a good approximation, the refractive index can be expressed as a function of density as

$$[n(z) - 1] / \rho(z) = [n(0) - 1] / \rho(0)\,. \quad (2.61)$$

Substituting Eq. (2.61) into Eq. (2.60) we get an equation in terms of the refractive index at sea level as follows:

$$[n(z)/n(z_i)]^2 = 1 + 2[n(0) - 1][\rho(z)/\rho(0) - \rho(z_i)/\rho(0)]\,. \quad (2.62)$$

The refractive index is determined using the dispersion formula of Edlen (1953) for the refractive modulus $N(0)$ at 15 degrees Celsius sea level appropriate for a density of 1.2250 $kg\ m^{-3}$ (the standard atmosphere sea level density),

$$N(0) = 64.328 + 29498.10/(146 - 1/\lambda^2) + 255.40/(41 - 1/\lambda^2)\,, \quad (2.63)$$

where λ is in μm. The refractive modulus is related to the index of refraction by

$$N(0) = [n(0) - 1]1E6\,. \quad (2.64)$$

Computations of relative airmass were made for sea level and 6 kilometers altitude using density values based on the *U. S. Standard Atmosphere* (1976) and the warmest and coldest supplementary atmospheres in the *U. S. Standard Atmosphere Supplements* (1966). The density at each altitude was obtained by truncated Chebyshev expansion using coefficients for the atmospheres between 0 and 80 kilometers *U. S. Standard Atmosphere Supplements* (1966) Tables 4.2, 4.3, 4.6, and 4.11). Computations for the standard atmosphere for 0 to 200 kilometers agreed within 1 percent with the results for 0 to 80 kilometers, therefore the results reported in Table 2.1 are for 0 to 80 kilometers for all three atmospheres.

The computations were made for a wavelength of 700 nanometers. Gast *et al.* (1965) indicate less than a 1 percent change in relative air mass for even a 90 degree zenith angle for wavelengths from 300 to 3000 nanometers. The values in Table 2.1 for the standard atmosphere at sea level agree within 0.1 percent of the Gast *et al.* (1965) values for 700 nanometers except at 90 degrees where they agree within 0.9 percent.

Table 2.1 presents values of relative optical airmass for angles 70 to 90 degrees. From 0 to 70 degrees, the relative airmass is equal to $sec\theta$ within 1 percent. The 45 degree North Spring/Fall values are appropriate for the *U. S. Standard Atmosphere* (1976). For purposes of comparison, the values for Bemporad from Gast *et al.* (1965) are given in Column 2 and for Kasten (1965) in Column 3. Bemporad assumed a sea level temperature of 0 degrees Celsius and a wavelength of 540 nanometers. Kasten used the ARDC (1959) densities which are essentially equivalent to the *U. S. Standard Atmosphere* (1976) and a wavelength of 700 nanometers.

Our computations compare well to the Kasten (1965) values except at zenith angle 90 degrees. Since his 90 degree value is also at odds with the Gast *et al.* (1965) values, his 90 degree approximation technique may be inadequate (there are special computational problems at 90 degrees). Bemporad's values lie as expected between the 45 degree Spring/Fall values and the 60 degree North (cold) values as does his ground level temperature.

Table 2.1. Relative optical air mass.

Selected Zenith Angles θ (degrees)	Sensor at Sea Level $m_{oo}(0,\theta)/m_{oo}(0,0°)$					Sensor at 6 Kilometers $m_{oo}(6,\theta)/m_{oo}(6,0°)$		
			From Std. Atmos 1976			From Std. Atmos 1976		
	Bemporad	Kasten	30° N July	45° N Spring/Fall	60° N Jan (cold)	30° N July	45° N Spring/Fall	60° N Jan (cold)
70	2.904	2.902	2.900	2.902	2.903	2.902	2.903	2.904
75	3.82	3.811	3.808	3.811	3.815	3.811	3.813	3.815
76	4.07	4.069	4.065	4.068	4.074	4.069	4.072	4.074
77	4.37	4.364	4.360	4.364	4.371	4.365	4.368	4.371
78	4.72	4.707	4.702	4.707	4.715	4.709	4.712	4.716
79	5.12	5.109	5.102	5.108	5.119	5.110	5.115	5.120
80	5.60	5.585	5.575	5.584	5.598	5.587	5.593	5.600
81	6.18	6.158	6.145	6.157	6.176	6.161	6.169	6.178
82	6.88	6.859	6.841	6.857	6.883	6.862	6.874	6.886
83	7.77	7.733	7.708	7.731	7.768	7..39	7.755	7 772
84	8.90	8.851	8.814	8.848	8.903	8.859	8.883	8.908
85	10.39	10.322	10.265	10.318	10.402	10.334	10.372	10.411
86	12.44	12.327	12.234	12.320	12.459	12.345	12.411	12.473
87	15.36	15.180	15.017	15.167	15.418	15.209	15.330	15.441
88	19.79	19.460	19.155	19.436	19.940	19.506	19.755	19.972
89	26.96	26.315	25.684	26.260	27.451	26.374	26.947	27.438
89.5		31.390	30.437	31.285	33.303	31.447	32.348	33.135
90	39.7	36.265	36.537	37.756	41.359	37.904	39.297	40.555
Wavelength (nm)	540	700	700	700	700	700	700	700
Temperature (°C)	0	15	31.43	15	-15.87	-6.63	-23.96	-38.99

In order to evaluate the effect of sensor altitude on the relative air mass, the 6 kilometer values are divided by the sea level values and the ratio given in Table 2.2 for 86 to 90 degrees. The relative airmass values agree for 6 kilometers with the sea level values within 1 percent from 70 to 86 degrees regardless of temperature. The largest altitude difference is +4.1 percent for the U.S. Standard Atmosphere at 90 degrees zenith angle. Altitude affects the relative airmass less than 1 percent for the coldest atmosphere except at 90 degrees (the temperature difference 0 to 6 kilometers is also smallest for the 60 degree North (cold) atmosphere).

The effect of temperature on the relative airmass is evaluated by ratioing the warmer and colder atmosphere values to the Standard Atmosphere values at 45 degrees North in Table 2.2. The effect of temperature is generally greater than the effect of sensor altitude. Also the effect of temperature is greater at sea level than at 6 kilometers.

Table 2.2. Altitude and temperature effects upon relative optical airmass.

Sun Zenith Angle θ_s (degrees)	ALTITUDE EFFECTS "6 km to Sea-Level" Ratios			TEMPERATURE EFFECTS "Warm-Cold to Standard" Ratios			
				Sea Level		6 Kilometers	
	30° July	45° Spring/Fall	60° Jan (cold)	30° N / 45° N	60° N / 45° N	30° N / 45° N	60° N / 45° N
86	1.009	1.007	1.001	.993	1.011	.995	1.005
87	1.013	1.012	1.001	.990	1.017	.992	1.007
88	1.018	1.016	1.002	986	1.026	.987	1.011
89	1.027	1.026	1.000	.978	1.045	979	1.018
89.5	1.033	1.034	995	.973	1.065	.972	1.024
90	1.037	1.041	981	.968	1.095	.965	1.032

Horizon Sky Equilibrium Radiance

As can be seen from Eq. (2.57) when the transmittance $T_\infty(z,90)$ is negligible, the horizon sky radiance is equal to the equilibrium radiance. In order to determine the minimum vertical transmittance necessary to produce a horizon sky radiance at equilibrium let us rearrange Eq. (2.58) as follows

$$\ln T_\infty(z,0) = \ln T_\infty(z,90) / [m_\infty(z,90) / m_\infty(z,0)] \ . \quad (2.65)$$

For 3 percent accuracy, $T_\infty(z,90)$ would be 0.03, then solving Eq. (2.65) using the relative airmass value for the standard atmosphere, we find that $T_\infty(z,0) = 0.911$. Thus for all vertical transmittances 0.911 or less, the horizon sky will be the equilibrium radiance to an accuracy of 3 percent or better. The Rayleigh transmittance for a wavelength of 555 nanometers for the Standard Atmosphere is 0.910. Thus for all wavelengths 555 nanometers or smaller, the horizon sky radiance will always be equal to the equilibrium radiance at sea level. Since the photopic has been found to be similar to the narrow band measurements at 555 nanometers, the photopic horizon sky radiance at sea level is also always reasonably equal to the equilibrium radiance for non-cloudy days.

The Rayleigh horizontal transmittance at 6 kilometers can be related to the vertical sea level transmittance by

$${}_R T_\infty(6,90) = {}_R T_\infty(0,0)^{m_\infty(6,90)/m_\infty(0,0)} \ . \quad (2.66)$$

Values of absolute vertical airmass, and relative vertical airmass for sea level and 6 kilometers are given in Table 2.3 for the same three atmospheres as in Table 2.1. Since

$$m_\infty(6,90)/m_\infty(0,0) = \frac{m_\infty(6,90)}{m_\infty(6,0)} \frac{m_\infty(6,0)}{m_\infty(0,0)} \ . \quad (2.67)$$

We now have the basis for evaluating Eq. (2.66). Using an equation similar to Eq. (2.65), we can now evaluate the vertical Rayleigh sea level transmittance necessary to produce a horizon sky radiance at 6 kilometers equal to the equilibrium radiance to an accuracy of 3 percent. This turns out to be $T_\infty(0,0) = 0.826$. Since the Rayleigh transmittance for 465 nanometers wavelength for the Standard Atmosphere is 0.823, the horizon sky radiances at 6 kilometers for wavelengths 465 nanometers or less will always be at equilibrium in cloudless skies.

2.4 Integrating the Equation of Transfer for Irradiance

The equation of transfer for irradiance Eq. (2.35) can be rearranged so that both sides can be integrated with respect to altitude. The limits of integration are between z_0 and z as we descend into the atmosphere so that z_0 is greater than z,

$$\int_{\xi(z_0)}^{\xi(z)} d\xi(z) = \int_{z_0}^{z} a(z)[m(\lambda,T) - \epsilon(z)]dz \ . \quad (2.68)$$

The left hand term is easily integrated but the right hand term is not. Partially integrated Eq. (2.68) becomes

$$\xi(z) - \xi(z_0) = \int_{z_0}^{z} a(z)[m(\lambda,T) - \epsilon(z)]dz \ . \quad (2.69)$$

Approximate Solution

A reasonable approximation to the integration can be obtained if we assume that the change in the difference $[m(\lambda,T) - \epsilon(z)]$ is small enough from z_0 to z such that an average value $[\overline{m(\lambda,T) - \epsilon(\Delta z)}]$ can be substituted. Substituting in the average scalar irradiance and exitance difference which can now be taken out of the integral we get

$$\xi(z) - \xi(z_0) = [\overline{m(\lambda,T) - \epsilon(\Delta z)}] \int_{z_0}^{z} a(z)dz \ . \quad (2.70)$$

The integral of the absorption with altitude is the optical thickness due to absorption ${}_a l_{\Delta z}(z)$ therefore

$$\xi(z) - \xi(z_0) = {}_a l_{\Delta z}(z) [\overline{m(\lambda,T) - \epsilon(\Delta z)}] \ . \quad (2.71)$$

Table 2.3. Temporal and latitudinal comparisons of vertical optical airmass.

Latitude and Season	ABSOLUTE AIR MASS at Sea Level $m_\infty(0,0^\circ)$ kg/m^2	ABSOLUTE AIR MASS at 6 km $m_\infty(6,0^\circ)$ kg/m^2	RELATIVE AIRMASS Altitude Ratio $m_\infty(6,0)/m_\infty(0,0^\circ)$
30° N July	1.03734E4	5.05429E3	.4872
45° N Spring/Fall	1.03566E4	4.83675E3	.4670
60° N Jan	1.034437E4	4.56196E3	.4410

* The notation E4 is equivalent to 10^4

The error in the resultant optical thickness is probably less than the variability of the difference $[m(\lambda,T)-\epsilon(z)]$ from the average value. This is an approximate equation for the net irradiance change with altitude.

An expression for the absorption optical thickness can be obtained by rearranging Eq. (2.71)

$$a\tau_{\Delta z} = [\xi(z) - \xi(z_0)] / [\overline{m(\lambda,T) - \epsilon(\Delta z)}] . \quad (2.72)$$

Thus if one has a measure of ambient temperature and downwelling, upwelling and scalar irradiance at two altitudes z_0 and z where z_0 is greater than z, the absorption optical thickness can be obtained.

No Absorption. When there is no absorption and hence no emission, Eq. (2.71) becomes

$$\xi(z) - \xi(z_0) = 0 \quad (2.73)$$

or substituting in Eq. (2.34)

$$E(z,d) - E(z,u) = E(z_0,d) - E(z_0,u) . \quad (2.74)$$

When there is no absorption the net irradiance does not change with altitude.

The albedo $A(z)$ is defined as the ratio of the upwelling to the downwelling irradiance,

$$A(z) = E(z,u) / E(z,d) . \quad (2.75)$$

Substituting Eq. (2.75) into Eq. (2.74) we get an expression in terms of downwelling irradiance and the albedo

$$E(z,d)[1 - A(z)] = E(z_0,d)[1 - A(z_0)] . \quad (2.76)$$

Thus the apparent albedo change with altitude is directly linked to the downwelling irradiance change with altitude when there is no absorption.

The albedo out-of-the-atmosphere $A(\infty)$ can be computed when the albedo and the downwelling irradiance at altitude z are known since the downwelling irradiance out of the atmosphere is the solar scalar irradiance ${}_s\epsilon(\infty)$ times the cosine of the sun zenith angle

$$E(\infty,d) = {}_s\epsilon(\infty)\cos\theta_s . \quad (2.77)$$

Substituting Eq. (2.77) into Eq. (2.76) and rearranging we get

$$A(\infty) = 1 - E(z,d)[1 - A(z)] / [{}_s\epsilon(\infty)\cos\theta_s] . \quad (2.78)$$

For example, if we assume the photopic clear day to have negligible absorption, we can use the illuminances from Brown (1952) to compute the albedo out of the atmosphere assuming various albedos at ground level. Using ${}_s\epsilon(\infty) = 1.89E3\ W/m^2\mu m$ and the Brown (1952) illuminances converted to irradiance in the same units (see Appendix A for details on the photopic as a broadband sensor), the results are shown in Table 2.4 and Fig. 2-4 for various ground level albedos. Ground level albedo $A(0)$ equal to 0.1 is probably the most reasonable in relation to the Brown (1952) illuminances.

Table 2.4. Albedo out-of-the-atmosphere for a non-absorbing atmosphere based on Brown (1952) and Eq. (2.78).

Sun Zenith Angle θ_s (degrees)	Downwelling Irradiance from Brown ('52) ($W/m^2\mu m$)	ALBEDO OUT-OF-THE-ATMOSPHERE, $A(\infty)$				
		Selected Ground Albedos, $A(0)$				
		0	0.1	0.2	0.8	1.0
0	1.70E3	0.101	0.190	0.280	0.820	1.0
40	1.17E3	0.192	0.273	0.354	0.838	1.0
60	6.47E2	0.315	0.384	0.452	0.863	1.0
80	1.51E2	0.540	0.585	0.632	0.908	1.0

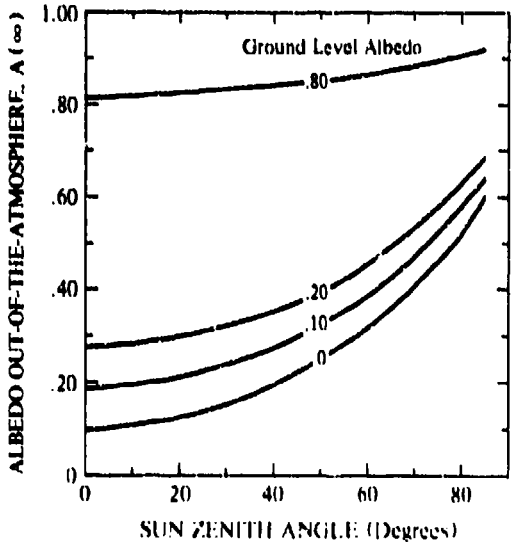

Fig. 2-4. Albedo out-of-the-atmosphere for a non-absorbing atmosphere, based upon Brown (1952) and Eq.(2.78).

Integrating for Scalar Irradiance

The equation of transfer for scalar irradiance Eq. 2.40 can be integrated by first dividing both sides by $\epsilon(z)$. Now multiplying by dz and integrating from z_0 to z where z_0 is greater than z as we descend into the atmosphere,

$$\int_{\epsilon(z_0)}^{\epsilon(z)} d\epsilon(z)/\epsilon(z) = -\int_{z_0}^{z} a(z) \int_{4\pi} \frac{L(z,\theta,\phi)}{\epsilon(z)} \sec\theta\, d\Omega\, dz . \quad (2.79)$$

Again the left hand term is easily integrated but the right hand is not. Let us define a function $D(z)$ which is a semi-normalized function of the 4π radiance distribution at altitude z

$$D(z) = \int_{4\pi} L(z,\theta,\phi)\sec\theta d\Omega \,/\, e(z) \,. \qquad (2.80)$$

The $D(z)$ is the unitless weighting function for the integral of absorption with altitude as it affects the change of scalar irradiance with altitude. An alternate way of expressing Eq. (2.80) is to separate out the sun term and to express the more diffuse radiances as a radiance difference, sky minus terrain as in Eq. (2.41)

$$D(z) = \sec\theta_s \, {}_s e(z)/e(z) + \int_{2\pi} [L(z,\theta',\phi') - L(z,\pi-\theta',\phi')]\sec\theta' d\Omega \,/\, e(z) \,. \qquad (2.81)$$

The first term is exact but the second term at large zenith angles becomes an approximation since $\sec\theta'$ becomes very large near 90 degrees. Fortunately, at 90 degrees, ΔL is zero.

Now substituting Eq. (2.80) into Eq. (2.79) and integrating the lefthand side we get

$$\ln [e(z)/e(z_0)] = -\int_{z_0}^{z} a(z) D(z) dz \,. \qquad (2.82)$$

This is the partially integrated equation for the change of scalar irradiance with altitude.

Approximate Solution. A reasonable approximation to the integration can be obtained if we assume that the change in $D(z)$ is small between z_0 and z so that an average value $\bar{D}(\Delta z)$ can be substituted

$$\ln [e(z)/e(z_0)] = -\bar{D}(\Delta z) \int_{z_0}^{z} a(z) dz \,. \qquad (2.83)$$

or in terms of the absorption optical thickness

$$\ln [e(z)/e(z_0)] = -\bar{D}(\Delta z) \, {}_a t_{\Delta z}(z) \,. \qquad (2.84)$$

The error in the resultant optical thickness is again probably less than the variability of the $D(z)$ from the average. This is an approximate solution for the change of scalar irradiance with altitude.

In order to obtain a measure of absorption optical thickness between two altitudes, we would rearrange Eq. (2.84) thus

$${}_a t_{\Delta z}(z) = \ln [e(z_0) / e(z)] / \bar{D}(\Delta z) \,. \qquad (2.85)$$

Equation (2.85) indicates that one needs a measurement of the 4π radiance distribution at both altitudes in order to compute the scalar irradiance and the radiance distribution function $D(z)$.

Water as a Scattering and Absorbing Medium. As an interesting and illustrative aside, one may consider the application of the foregoing equations within the hydrological context. Although the principal emission mechanism in water is thermal there is also bioluminescence. Bioluminescence is essentially chemiluminescence, that is, energy from chemical reaction instituted by biological organisms. It is also isotropic. Thus in water the total emittance path function is $L_{*_e}(d) = L_{*_a}(d) + L_{*_b}(d)$. In water the radiances are denoted in terms of the depth d beneath the water surface rather than the height above the sea floor z. Since the path function due to bioluminescence is isotropic, the equation of transfer for scalar irradiance Eq. (2.40) is appropriate for water whether bioluminescence is present or not. On the other hand, the equation of transfer for irradiance Eq. (2.35) only applies to water when bioluminescence is not present, otherwise, a bioluminescent term must be added. Also in the visible spectrum in water, thermal emission is negligible as it is in the troposphere. In water, below a certain depth d_1 the light distribution becomes asymptotic, with the sun no longer a separate component. Thus the function $D(d_1)$ which is solely a function of the lighting distribution becomes a constant and can be expressed as the right hand term of Eq. (2.81)

$$D(d_1) = \int_{2\pi} [L(d_1,\theta',\phi') - L(d_1,\pi-\theta',\phi')]\sec\theta' d\Omega \,/\, e(d_1). \qquad (2.86)$$

Also at depth d_1 and below, absorption is constant. Therefore the equation of transfer for scalar irradiance Eq. (2.79) becomes

$$\int_{e(d_0)}^{e(d)} de(d)/e(d) = -a\, D(d_1) \int_{d_0}^{d} dd \,. \qquad (2.87)$$

This is easily integrated with depth to become

$$\ln [e(d)/e(d_0)] = -\, a\, D(d_1)(d - d_0) \,, \qquad (2.88)$$

where d_0 must be at or below d_1 the depth at which the lighting distribution becomes asymptotic.

In water, the constant k is defined as [Eq. 7 Section 1.2 Vol. I Preisendorfer (1976)]

$$\ln[e(d)/e(d_0)] = -k(d-d_0) \,. \qquad (2.89)$$

Therefore Eq. (2.88) together with Eq. (2.89) give us an equation for k in terms of the absorption a and the

asymptotic lighting distribution function D defined by Eq. (2.86),

$$k = aD(d_1) \quad . \tag{2.90}$$

Thus, having noted the conceptual similarities between the hydrosphere and atmosphere, our discussion returns to the subject at hand, the atmosphere as a radiative transfer medium.

Discussion

Equations (2.71) and (2.84) which describe net irradiance and scalar irradiance are essentially three dimensional. They address the effect of absorption over an area as well as vertically. They do not assume homogeneity but they do assume a relatively small change in $m(\lambda,T)-\epsilon(z)$, and $D(z)$ over the altitude interval. Thus clouds may be present and the equations can still be valid. The equations assume z_o is vertically above z and describe a single point in time.

When there are clouds in the altitude increment Δz, Eq. (2.85) should indicate absorption. This is an absorption based on the 4π lighting distribution. Thus, even if there is no absorption in the direction of the sun, the presence of clouds will affect the 4π lighting distribution and absorption should be indicated.

We now have two equations Eq. (2.72) and (2.84) to obtain the absorption optical thickness. Therefore it should be possible to use them simultaneously as a check on the efficacy of the approximate solutions, that is

$$a'_{\Delta z}(z) = [\,\xi(z) - \xi(z_o)\,] \,/\, [\,\overline{m(\lambda,T) - \epsilon(\Delta z)}\,]$$
$$= \ln [\epsilon(z_o) \,/\, \epsilon(z)] \,/\, \bar{D}(\Delta z) \quad . \tag{2.91}$$

Visible Spectrum. In the visible spectrum, the emission is negligible therefore Eq. (2.91) simplifies to

$$a'_{\Delta z}(z) = [\xi(z_o) - \xi(z)] \,/\, \bar{\epsilon}(\Delta z)$$
$$= \ln [\epsilon(z_o) \,/\, \epsilon(z)] \,/\, \bar{D}(\Delta z) \quad . \tag{2.92}$$

The above equations are monochromatic. They are, however, reasonable engineering approximations for a broadband sensor when the absorption is primarily in broadband continua or due to the suspended particles or water droplets and not line or band spectra. This holds reasonably well in the atmosphere in the visible portion of the spectrum.

To test Eq. (2.92) and to get an understanding of the lighting distribution function $D(z)$, we used the sky and terrain radiances measured for Filter 2 mean wavelength 478 nanometers on flight C-466 in Meppen, Germany on 15 August 1978 during project OPAQUE V described in Johnson and Gordon (1980). The altitude z_o was chosen as the highest altitude flown 6 kilometers and the z used was for the lowest altitude flown 0.2 kilometers. Thus Δz equals 5.8 kilometers. The sun was unobscured at both altitudes but there were scattered cirrus clouds.

The first step was to correct the scanner data in the region 0 to 25 degrees scattering angle from the sun. Recent scanner tests indicate spurious sun reflection in sky radiance measurements near the sun. The method used was similar to the Barteneva (1960) method for extrapolating the volume scattering function near scattering angle 0 degrees. We assumed log sky radiance at each zenith angle to be linear with $\cos\beta$ from 0 to 30 degrees. The slope of the line was established by the values near 30 degrees scattering angle.

The next step was to obtain a measure of radiance transmittance appropriate for the unobscured sun. This was done using the solar almucantar sky radiances in a method described later in Section 4.6.

As a check, the resultant computed downwelling irradiances were compared to the irradiometer measurements. The irradiances computed from the sky-terrain scanner measurements are given in Table 2.5 together with the ratios to the irradiometer values. The computed downwelling irradiances compare as well or better than the upwelling irradiances and thus the corrected sky radiances were considered reasonable.

For computing the radiance distribution function $D(z)$, Eq. (2.81) was rewritten as

$$D(z) = \sec\theta_s \, s\epsilon(z) / \epsilon(z)$$
$$+ 2\pi \int_o^{\pi/2} [\bar{L}(z,\theta') - \bar{L}(z,\pi-\theta')] \sec\theta' d\theta' \,/\, \epsilon(z) \quad . \tag{2.93}$$

The average radiance $\bar{L}(z,\theta')$ for each zenith angle was computed by summing the radiances for all 60 azimuths and dividing by 60. The resultant average radiance differences $\bar{L}(z,\theta')-\bar{L}(z,\pi-\theta')$ are graphed in Fig. 2-5.

The computations of the distribution function $D(z)$ using Eq. (2.93) are given in Table 2.6. Note that the second or sky-terrain term is relatively small (23 percent of the total) at high altitude but more than half the total at low altitude.

The evaluation of Eq. (2.92) is also shown in Table 2.6 together with the average absorption optical thickness based on an average of the values using the two methods. The average differs from the individual evaluations by ±9 percent. This compares well to the estimate of error for each value. The estimated error for Eq. (2.72) is ±8 percent based on the variability of the difference $[m(\lambda,T)-\epsilon(z)]$ from the average. Whereas the estimated error for Eq. (2.85) is 14.7% based on the variability of $D(\Delta z)$ from the average value.

The resultant absorption optical thickness probably errs on the high side since no attempt was made to correct for the small sun zenith angle change between the measurements at 6 kilometers and 0.2 kilometers.

The above is too small a sample to validate the method but is encouraging enough to indicate further development might prove fruitful.

Table 2.5a. Computed scalar irradiances for flight C-466, filter 2 $\bar{\lambda} = 478nm$.

SPECIFIC IRRADIANCE COMPONENT	COMPUTED SCALAR IRRADIANCES ($W/m^2\mu m$)			
	At 6km $\epsilon(6)$	At .2km $\epsilon(.2)$	Average Over Altitude $\bar{\epsilon}(\Delta z)$	Change Over Altitude $\ln[\epsilon(z_0)/\epsilon(z)]$
Sun $_s\epsilon(z)$	1796	1113		
Sky $_d\epsilon(z,d)$	338	838		
Upwelling $\epsilon(z,u)$	424	227		
Total $\epsilon(z)$	2558	2178	2368	.1608
Albedo $_sA$	.109	.119		

Table 2.5b. Computed flat plate irradiances for flight C-466, filter 2, $\bar{\lambda} = 478\,nm$.

SPECIFIC IRRADIANCE COMPONENT	COMPUTED FLAT PLATE IRRADIANCES ($W/m^2\mu m$)	
	At 6 km $E'(6)$ Calculated from Scanner	At 2km $E'(.2)$ Calculated from Scanner
Sun $_sE'(z)$	1359	757
Sky $_dE'(z,d)$	114	380
Total Downwelling $E'(z,d)$	1473	1137
Total Upwelling $E'(z,u)$	187	77
Albedo, $A(z)$	127	.069
Net $\xi(z)$	1286	1060
Calculated-Measured Ratios		
Downwelling (Scan/Irrad)	1.04	1.02
Upwelling (Scan/Irrad)	0.96	1.11

Table 2.6a. Lighting distribution function D(z) from Eq. (2.93), flight C-466, filter 2, $\bar{\lambda} = 478\,nm$.

Specific Distribution Component	DISTRIBUTION FUNCTION D(z) At 6km D(6)	At .2km D(.2)
Sun	0.928	0.751
Sky-Terrain	0.274	0.865
Total	1.202	1.616
Average $\bar{D}(\Delta z)$	1.409	

Table 2.6b. Comparison of absorption optical thickness determinations.

Computational Procedure	Computed Absorption Optical Thickness $_a\tau_{5.8}(.2)$
From Net Irradiance Eq. (2.72)	0.0954
From Scalar Irradiance Eq. (2.85)	0.1141
Average Value	0.1048

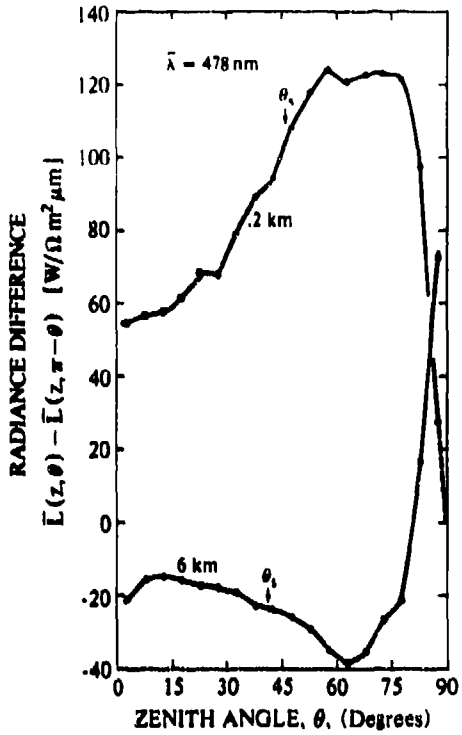

Fig. 2-5. Average radiance difference $\bar{L}(z,\theta)-\bar{L}(z,\pi-\theta)$ for flight C-466, filter 2 ($\bar{\lambda}$ = 478 *nm*).

Table 2.7. Ratio of incremental path length $\Delta r(z_i)/\Delta r(z)$ for Δz = 30 meter increments for both upward and downward paths of sight between ground level (z = 0) and 6 km (z = 6).

Zenith Angle # (degrees)	Upward Paths of Sight $\Delta r(6)/\Delta r(0)$	Zenith Angle # (degrees)	Downward Paths of Sight $\Delta r(0)/\Delta r(6)$
70	.994	110	1.006
75	.989	105	1.012
76	.987	104	1.013
77	.985	103	1.016
78	.982	102	1.019
79	.979	101	1.022
80	.975	100	1.027
81	.969	99	1.034
82	.961	98	1.044
83	.950	97	1.059
84	.934	96	1.083
85	.908	95	1.127
86	.866	94	1.225
87	.792	93	1.569
88	.654		
89	.397		

Earth Curvature Effects

The above equations were developed for a plane parallel atmosphere. Refraction and earth curvature effects were ignored. However, for upward and downward paths of sight between 6 kilometers and ground level, the incremental path length Δr_i is affected to a significant extent by earth curvature and refraction for the longer slant paths of sight. For these paths of sight, the incremental path length Δr is computed from Eq. (2.19).

As indicated earlier, the Δr for a constant Δz is shorter at altitude than at ground level for upward paths at zenith angles greater than 70 degrees, and longer at ground level than at altitude for downward paths of sight less than 110 degrees in zenith angle. The ratio of the incremental path length at ground level and 6 kilometers for these paths is given in Table 2.7. The Δr values were computed from Eq. (2.19) for a refractive index appropriate for a wavelength of 700 nm and standard atmosphere densities. There is no ratio for zenith angles 92 and 91 degrees since at these angles the path of sight does not intersect the surface of the earth due to earth curvature.

The Δr at the sensor position is equivalent to $sec\theta$. It is the Δr at the beginning of the flux path that departs from $sec\theta$ by the ratios indicated in Table 2.7. These ratios indicate the maximum error in using $sec\theta$ for these angles for paths between 0 and 6 km. The error is less than 3 percent for paths from 70 to 80 and 100 to 110 degrees.

For paths from 80 to 100 degrees, it is appropriate to compute the relative airmass to compare to $sec\theta$. The absolute airmass was computed using Eq. (2.59) integrating from 0 to 6 km. Values of relative airmass, and the ratios to $sec\theta$ for selected zenith angles from 80 to 100 degrees are given in Table 2.8. Use of $sec\theta$ to obtain Δr for a 6 kilometer altitude increment introduces an error of +1.1 to +4.5 percent for 80 to 85 degrees zenith angle and an error of -1.5 to -6.3 percent for 95 to 100 degrees. This is small enough to be neglected. However, at 87 degrees the error is +11.6 percent and at 93 degrees the error is -20.2 percent.

Checking back into the computations we found that the contribution to $D(z)$ at zenith angle 87.5 degrees is large at high altitude, essentially all of the second term. Whereas at low altitude the radiance difference at 87.5 degrees is less relative to the other zenith angles so that it comprises only 18 percent of the second term or 10 percent of the total. The contribution of the radiance difference at 87.5 degrees is probably the most questionable part of the evaluation of the distribution function $D(z)$. Thus the uncertainty of $D(6km)$ is on the order of 23 percent and of $D(0.2km)$ is 10 percent.

Table 2.8. Comparison of relative optical airmass, $m_r(z,\theta)/m_r(z,0)$ to $sec\theta$ (computed using Δz = 30 meters for vertical path of 6 km).

UPWARD PATHS OF SIGHT				DOWNWARD PATHS OF SIGHT			
Zenith Angle θ_s (degrees)	$sec\theta$	Relative Airmass $\frac{m_r(0,\theta)}{m_6(0,0)}$	Ratio $\frac{sec\theta}{Rel.\ Airmass}$	Zenith Angle θ_s (degrees)	$-sec\theta$	Relative Airmass $\frac{m_r(6,\theta)}{m_6(6,180)}$	Ratio $\frac{-sec\theta}{Rel.\ Airmass}$
80	5.759	5.694	1.011	100	5.759	5.845	.985
85	11.474	10.982	1.045	95	11.474	12.244	.937
87	19.107	17.121	1.116	93	19.107	23.939	.798

3. SOLAR ALMUCANTAR

3.1 Sky Radiance

The almucantar is the part of the sky at a constant zenith angle, all azimuths. The solar almucantar is the sky at the zenith angle of the sun θ_s. The sky radiance in the solar almucantar is the path radiance out-of-the-atmosphere to the sensor at altitude z. The sky radiance can be expressed as

$$L_\infty^*(z,\theta_s,\phi) = \int_\infty^z L_*(z_l,\theta_s,\phi)\ T_{rl}(z,\theta_s)\,dr\ . \qquad (3.1)$$

The path function $L_*(z,\theta_s,\phi)$ can be expressed in terms of a sun component, a sky-terrain component and an emitted component

$$L_*(z,\theta_s,\phi) = {}_s\epsilon(z)\sigma(z,\beta) + \int_{4\pi} L(z,\theta',\phi')\sigma(z,\beta')\,d\Omega + L_{*_a}(z)\ . \qquad (3.2)$$

or

$$L_*(z,\theta_s,\phi) = {}_s\epsilon(z)\left[\sigma(z,\beta) + \int_{4\pi} L(z,\theta',\phi')\sigma(z,\beta')\,d\Omega/{}_s\epsilon(z) + L_{*_a}(z)/{}_s\epsilon(z)\right]\ . \qquad (3.3)$$

Let the last two terms be designated by the function $C(z)$ such that

$$C(z) = \int_{4\pi} L(z,\theta',\phi')\sigma(z,\beta')\,d\Omega/{}_s\epsilon(z) + L_{*_a}(z)/{}_s\epsilon(z)\ . \qquad (3.4)$$

Substituting Eqs. (3.3) and (3.4) into Eq. (3.1) we get

$$L_\infty^*(z,\theta_s,\phi) = \int_\infty^z {}_s\epsilon(z_l)\,T_{rl}(z,\theta_s)[\sigma(z_l,\beta) + C(z_l)]\,dr\ . \qquad (3.5)$$

The sun scalar irradiance and the transmittance can be expressed as a function of the sun irradiance out of the atmosphere ${}_s\epsilon(\infty)$ as follows

$${}_s\epsilon(z_l)T_{rl}(z,\theta_s) = {}_s\epsilon(\infty)\exp\left[-\int_\infty^{z_l}\alpha(z)\,dr - \int_{z_l}^{z}\alpha(z)\,dr\right]\ . \qquad (3.6)$$

The two integrals can be combined and expressed in terms of the limits ∞ to z which is equivalent to the total transmittance, thus

$${}_s\epsilon(z_l)T_{rl}(z,\theta_s) = {}_s\epsilon(\infty)T_\infty(z,\theta_s) = {}_s\epsilon(z)\ . \qquad (3.7)$$

Now substituting into Eq. (3.5), the sun irradiance can be taken out of the integral and we get

$$L_\infty^*(z,\theta_s,\phi)/{}_s\epsilon(z) = \int_\infty^z [(\sigma(z,\beta) + C(z)]\,dr\ . \qquad (3.8)$$

The quantity in the square brackets is a function of altitude and not of zenith angle, therefore

$$\int_\infty^z [\sigma(z,\beta) + C(z)]\,dr = [m_\infty(z,\theta_s)/m_\infty(z,0)]\int_\infty^z [\sigma(z,\beta) + C(z)]\,dz\ . \qquad (3.9)$$

where $m_\infty(z,\theta_s)/m_\infty(z,0)$ is the relative optical airmass at θ_s. For altitudes up to 6 kilometers we can use the sea level value for sun zenith angles 0 to 86 degrees so for convenience we will shorten this to $m(\theta_s)$. Substituting back into Eq. (3.8) we get

$$L(z,\theta_s,\phi)/[{}_s\epsilon(z)m(\theta_s)] = \int_\infty^z [\sigma(z,\beta) + C(z)]\,dz\ . \qquad (3.10)$$

The right hand term can be separated into two parts

$$\int_\infty^z [\sigma(z,\beta) + C(z)]\,dz = \int_\infty^z \sigma(z,\beta)\,dz + \int_\infty^z C(z)\,dz\ . \qquad (3.11)$$

Now let us define an optical thickness function $\tau_\infty(z,\beta)$ such that

$$\tau_\infty(z,\beta) = \int_\infty^z \sigma(z,\beta)\,dz \,. \tag{3.12}$$

The integral of the optical thickness function over 4π is the optical thickness due to scattering ${}_s t_\infty(z)$

$${}_s t_\infty(z) = \int_{4\pi} \tau_\infty(z,\beta)\,d\Omega \tag{3.13}$$

since the optical thickness due to scattering is the integral of the total scattering coefficient with altitude

$${}_s t_\infty(z) = \int_\infty^z s(z)\,dz \,. \tag{3.14}$$

Substituting Eq. (3.12) into Eq. (3.10) we get

$$L^*_\infty(z,\theta_s,\phi)/[{}_s\epsilon(z)\,m(\theta_s)] = \tau_\infty(z,\beta) + \int_\infty^z C(z)\,dz \,. \tag{3.15}$$

This is the basic equation for the radiance in the solar almucantar and how it relates to the sun scalar irradiance, the optical airmass, the optical thickness function and one additive component defined by Eq. (3.4).

3.2 Optical Stability

Transmittances from Solar or Solar Almucantar Radiances

The atmosphere is considered to be optically stable when the atmospheric transmittance does not change with time. When the day is optically stable, measurements of the apparent sun radiance ${}_s L_\infty(z,\theta_s,0)$ made over a large range of sun zenith angle can yield a good measure of total transmittance $T_\infty(z,0)$ and the inherent sun radiance ${}_s L_0(\infty)$

$${}_s L_\infty(z,\theta_s,0) = {}_s L_0(\infty)\,T_\infty(z,0) \,. \tag{3.16}$$

Taking the log of both sides of Eq. (3.16) we get

$$\log {}_s L_\infty(z,\theta_s,0) = \log {}_s L_0(\infty) + m(\theta_s) \log T_\infty(z,0) \,. \tag{3.17}$$

Graphs of apparent sun radiance on semi-log paper of log apparent sun radiance versus airmass yield the typical Langley (or Bouguer) graph where log inherent sun radiance is the intercept and log transmittance is the slope.

Variations of Eq. (3.15) give both another method for obtaining the total transmittance and several ways of checking the optical stability. Equation (3.15) can also be written as

$$L^*_\infty(z,\theta_s,\beta)/m(\theta_s) = T_\infty(z,0)^{m(\theta_s)}\,{}_s\epsilon(\infty)\left[\tau_\infty(z,\beta) + \int_\infty^z C(z)\,dz\right] \,. \tag{3.18}$$

Taking the log of both sides we get

$$\log[L^*_\infty(z,\theta_s,\beta)/m(\theta_s)] = m(\theta_s)\,\log T_\infty(z,0) + \log A \tag{3.19}$$

where

$$A = {}_s\epsilon(\infty)\left[\tau_\infty(z,\beta) + \int_\infty^z C(z)\,dz\right] \,. \tag{3.20}$$

For an optically stable day, A should be constant for a given angle from sun. Thus the sky radiance at a constant β in the solar almucantar can be used to obtain the beam transmittance when measured over a large range of airmass values on an optically stable day. A semi-log graph of $\log[L^*_\infty(z,\theta_s,\beta)/m(\theta_s)]$ versus airmass would be linear with a slope of log transmittance and an intercept at $\log A$. The transmittance obtained from the sun radiance using Eq. (3.17) and the transmittance obtained from the sky radiance in the solar almucantar are then averaged to obtain the most accurate value.

Tashenov (1970) used this method with measurements of the solar aureole to obtain spectral transmittance in the region 410 to 735 nanometers.

Tests to Determine Optical Stability

Pyaskovskaya-Fesenkova (1970) outlines two tests for optical stability as well as a unique equation for transmittance which is valid only for optically stable days.

The first test is to graph for a constant scattering angle the ratio $L^*_\infty(z,\theta_s,\beta)/[{}_s\epsilon(z)\,m(\theta_s)]$ versus $m(\theta_s)$. As can be seen from Eq. (3.15), if the day is optically stable the right hand term is constant. Therefore this graph should result in a horizontal straight line. That is, for an optically stable day

$$L^*_\infty(z,\theta_s,\beta)/[{}_s\epsilon(z)\,m(\theta_s)] = B \tag{3.21}$$

where

$$B = \tau_\infty(z,\beta) + \int_\infty^z C(z)\,dz \,. \tag{3.22}$$

The second test for optical stability is to graph the ratio $L^*_\infty(z,\theta_s,\beta)/{}_s\epsilon(z)$ versus relative airmass for a constant β. The graph should result in a straight line going through the origin on an optically stable day. To understand this, Eq. (3.15) is rewritten in the form

$$L^{\circ}_{\infty}(z,\theta_s,\beta)/{}_s\epsilon(z) = m(\theta_s)\ B\ . \qquad (3.23)$$

The B is now the slope and the intercept is zero.

If the day is optically stable a graph of solar almucantar radiance at a constant scattering angle versus airmass will yield a value of transmittance as follows. If we write Eq. (3.21) in the form

$$L^{\circ}_{\infty}(z,\theta_s,\beta) = {}_s\epsilon(\infty)\,T_{\infty}(z,0)^{m(\theta_s)}\ m(\theta_s)\ B \qquad (3.24)$$

and differentiate (only the sky radiance and the air mass are variables, the inherent sun scalar irradiance, B and the transmittance are constant), we get

$$dL^{\circ}_{\infty}(z,\theta_s,\beta)$$

$$= B\ {}_s\epsilon(\infty)\,T_{\infty}(z,0)^{m(\theta_s)}\ d\ m(\theta_s)[1+m(\theta_s)\ln T_{\infty}(z,0)]\ . \qquad (3.25)$$

Equation (3.25) is only valid when the angle from sun is constant, the vertical transmittance from space to sensor is constant and the day is optically stable. Setting $dL^{\circ}_{\infty}(z,\theta_s,\beta)$ equal to zero and rearranging we get

$$\ln T_{\infty}(z,0) = -1/m(\theta_s') \qquad (3.26)$$

where θ_s' is the sun angle where $L^{\circ}_{\infty}(z,\theta_s,\beta)$ is a maximum. Therefore a graph of solar almucantar radiance at a constant angle from the sun versus airmass will increase and then decrease with the maximum at $m(\theta_s')$ when the day is optically stable. If the curve is reasonably well defined with sufficient airmass values, a reasonable transmittance value can be obtained. It can also be used as a third test for optical stability. The values of transmittance obtained by means of Eqs. (3.17), (3.19) and (3.26) should be in agreement on an optically stable day.

Pyaskovskaya-Fesenkova (1970) describes an instrument for measuring the quantities in the preceding equations. It is essentially a radiance photometer with a three degree field of view for the solar measurement. For the aureole measurement a two degree to three degree circular zone is used. Her article also includes a theoretical test of the error in obtaining transmittance from the sun radiance when the aureole in the three degree field is necessarily a part of the sun radiance measurement. She concluded the error to be negligible.

3.3 Method of Determining Spurious Sun Reflectance

Pyaskovskaya-Fesenkova (1970) also indicates that the two methods of checking for optical stability will falsely indicate instability if reflections in the radiometer telescope are not negligible.

Conversely, once it is established that the day is optically stable, the above tests for optical stability can be used to test whether a sky radiance measurement contains spurious sun reflection. Sky radiances near the sun are difficult to measure unless the sun can be occulted. For example, recent tests made with the C-130 sky scanning photometer indicate spurious sun reflections in the measurements at scattering angles 0 to 25 degrees from the sun.

To illustrate the use of the above tests for optical stability and to test for spurious sun reflections in a sky radiance photometer, we will use a set of data containing measurements with a solar transmissometer, a sky scanner and an irradiometer. These measurements were made from January to September 1964 from a platform on the roof of one of the Visibility Laboratory buildings at Point Loma. The solar transmissometer measured both the center sun radiance and an aureole radiance 0.573 degrees from the sun center. The general procedure was to make a set of measurements at each 10 degree increment of sun zenith angle and at noon.

The photometers were fitted with four optical filters so that there were two narrow filtered-sensor passbands and two broad passbands. The two narrow passbands had mean wavelengths of 459 and 661 nanometers, the photopic passband had a mean wavelength of 560 nanometers, and a fourth broad passband represented an unfiltered sensor with a mean wavelength of 505 nanometers. Relative spectral response curves for these filters are given in Appendix A.

A graph of the apparent center sun radiance as a function of relative airmass for the afternoon of 2 September 1964 is given in Fig. 3-1. The straight lines for each filter are the result of least squares fits to the data. The correlation coefficients were high, equal to or greater than 0.99 and the day is apparently optically stable. The least squares transmittances are noted on the graph.

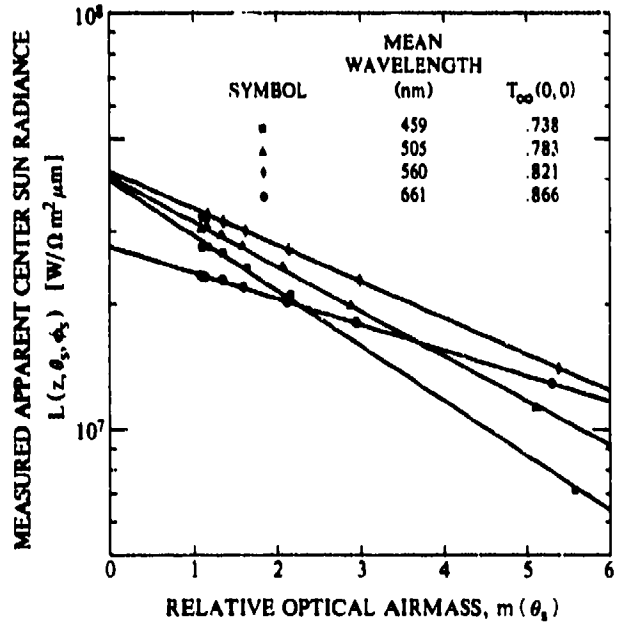

Fig. 3-1. Langley graph of measured apparent center sun radiance for 2 September 1964.

Solar Almucantar at 55 degrees

In order to be certain to have an almucantar sky radiance measurement without sun reflection problems, an angle from sun of 55 degrees was chosen. The sky scanner data are for a fixed set of zenith angles and azimuths ($\Delta\theta$ and $\Delta\phi$ = 5.625 degrees). Therefore the almucantar radiance used is from interpolations to the zenith angle of the sun and to the appropriate azimuth for β equal to 55 degrees. The example is done for only Filter 1 mean wavelength 459 nanometers. The almucantar/$m(\theta_s)$ graph versus airmass (Eq. (3.19)) is given in Fig. 3-2. The transmittance from the almucantar is 0.756 compared to the transmittance from the center sun radiance of 0.738 thus there is only a 2.4 percent difference. The average 0.747 is considered the best measure of the transmittance if the day is optically stable.

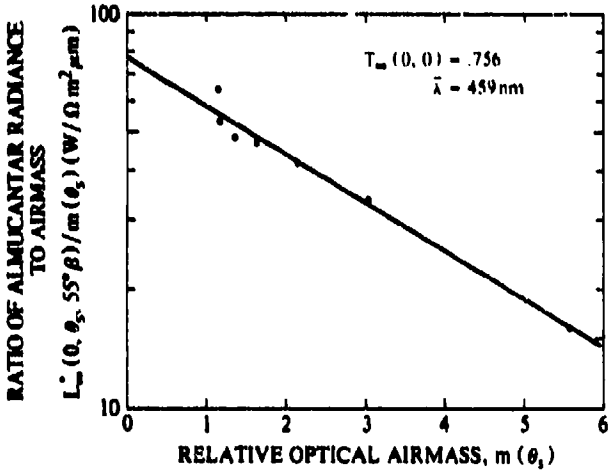

Fig. 3-2. Almucantar radiance to airmass ratio vs relative optical airmass for 2 September 1964.

Now for the three tests for optical stability. Although we do not have a measure of the solar scalar irradiance $_s e(0)$, we do have a center sun radiance $_s L_\infty(0,\theta_s,0)$ which is related to the scalar irradiance by

$$_s e(0) = {}_s L_\infty(0,\theta_s,0) D(\bar{\lambda}) \Omega_s , \qquad (3.27)$$

where $D(\bar{\lambda})$ is the center to average sun radiance conversion or limb darkening factor for the filter (see Appendix A) and Ω_s is the solid angle subtended by the sun for 2 September 1964. If we substitute the center sun radiance for the solar scalar irradiance in Eq. (3.21) we get

$$L^*_\infty(z,\theta_s,\beta)/[{}_s L_\infty(0,\theta_s,0) m(\theta_s)] = B' , \qquad (3.28)$$

where

$$B' = D(\bar{\lambda}) \Omega_s B . \qquad (3.29)$$

Similarly Eq. (3.23) becomes

$$L^*_\infty(z,\theta_s,\beta)/{}_s L_\infty(z,\theta_s,0) = m(\theta_s) B' . \qquad (3.30)$$

Since $D(\bar{\lambda})$ is a constant for a filter and Ω_s is constant for any given day, the two tests can now be made using Eqs. (3.28) and (3.30) instead of Eqs. (3.21) and (3.23).

Fig. 3-3 contains the appropriate graphs for the two tests. Although not perfect, the data in Fig. 3-3a is reasonably represented by a horizontal straight line. Similarly, the data in Fig. 3-3b are reasonably represented by a straight line going through the origin.

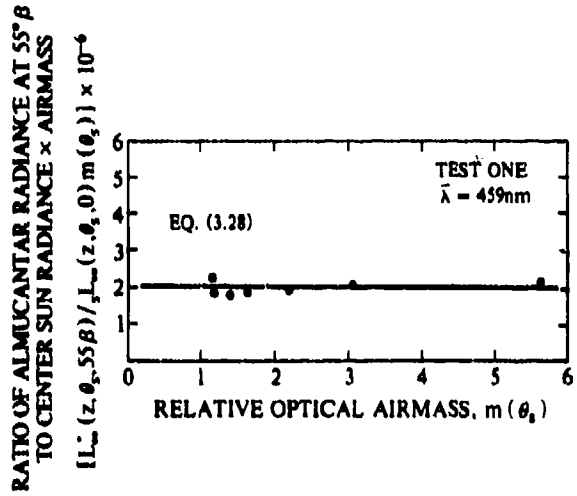

Fig. 3-3a. Graphs to test atmospheric optical stability for 2 September 1964, filter 1 ($\bar{\lambda}$ = 459 *nm*), Test One, Eq.(3.28).

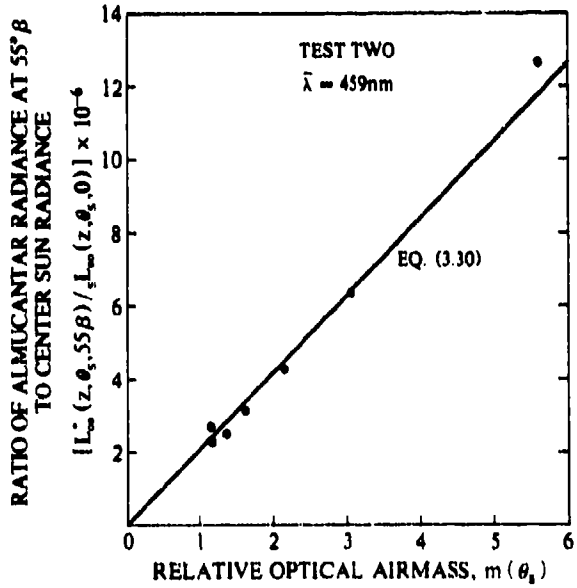

Fig. 3-3b. Graphs to test atmospheric optical stability for 2 September 1964, filter 1 ($\bar{\lambda}$ = 459 *nm*), Test Two, Eq.(3.30).

The third test is a plot of the almucantar sky radiance graphed against $\exp[-1/m(\theta_s)]$ from Eq. (3.26) as shown in Fig. 3-4. The maximum sky radiance should lie at a transmittance of approximately 0.75. Although the noon value of sky radiance is inconsistent with the rest (hooks upward near air mass one), and there are no meas-

ured sky radiances at the exact θ_s', the sky radiances can be reasonably represented by a curve which maximizes at a transmittance of 0.75 (dashed line).

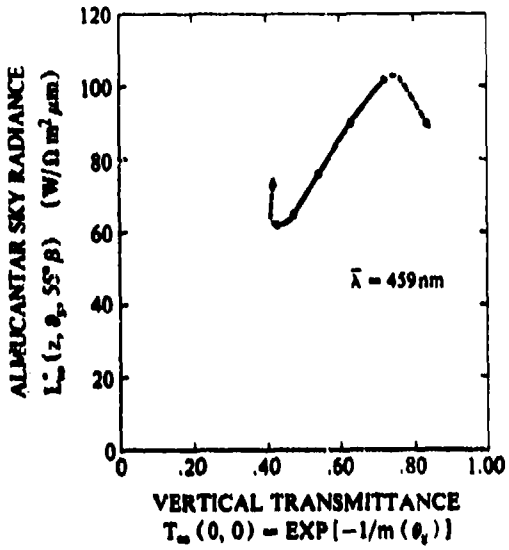

Fig. 3-4. Almucantar sky radiance at 55° vs vertical transmittance (Eq. 3.26) for 2 September 1964, filter 1 ($\bar{\lambda}$ = 459 *nm*).

Thus we conclude that the atmosphere on 2 September 1964 in the vicinity of the Visibility Laboratory was reasonably stable optically. Also we conclude that scanner radiances may be used to obtain almucantar values by interpolation for use in the preceding equations.

Now that it is established that the day is optically stable, we will use these same equations to test for sun reflections in the aureole photometer.

Aureole Radiance

The solar aureole radiance was measured 0.573 degrees from the center of the sun without occulting the sun. A graph of the ratio of the apparent aureole radiance to the relative airmass versus airmass is given in Fig. 3-5.

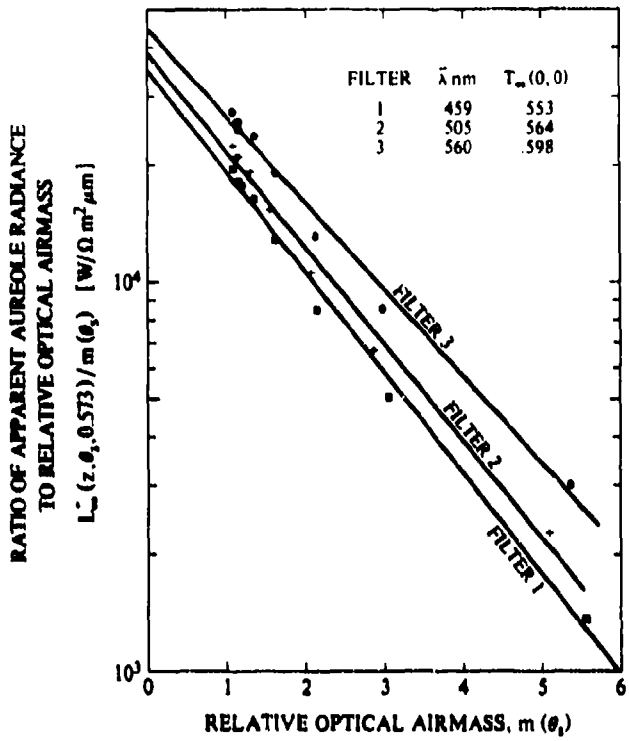

Fig. 3-5. Aureole radiance to airmass ratio vs relative optical airmass for 2 September 1964.

The data for the three filters look reasonably linear and the correlation coefficients are 0.99. However, the least squares transmittances, which are noted on the graph, vary markedly from the values derived from the sun radiance and the almucantar at 55 degrees scatterinig angle.

The two tests for spurious sun reflection using Eqs. (3.28) and (3.30), fail miserably, see Fig. 3-6a and b. In Fig. 3-6a the B' increases dramatically as airmass gets near one instead of staying constant. In Fig. 3-6b the data can be fit to straight lines but they clearly do not go through the origin.

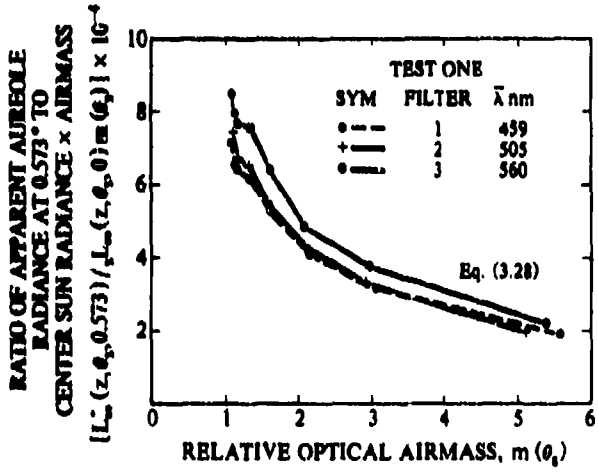

Fig. 3-6a. Graphs to test for spurious sun reflections in aureole radiance measurements, 2 September 1964, Test One, Eq.(3.28).

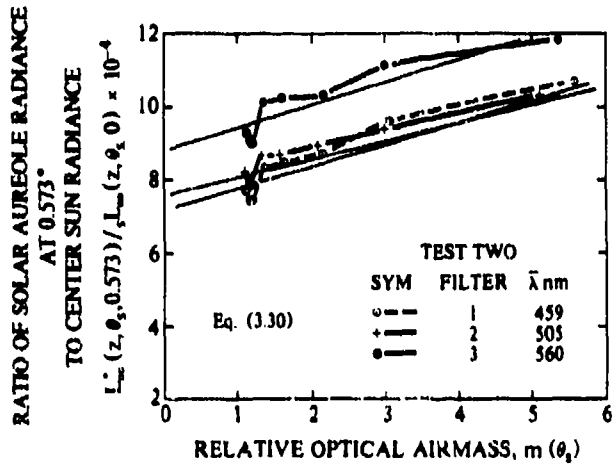

Fig. 3-6b. Graphs to test for spurious sun reflections in aureole radiance measurements, 2 September 1964, Test Two, Eq.(3.30).

The final test is the graph of the solar aureole radiance as a function of $\exp[-1/m(\theta_s)]$ as shown in Fig. 3-7. The aureole peaks at transmittances still lower than the values derived using the aureole and noted in Fig. 3-5. The transmittances from Eqs. (3.17), (3.19) and (3.26) are clearly not in agreement. Thus we conclude that the solar aureole measurements include a spurious sun reflection component in all three filters.

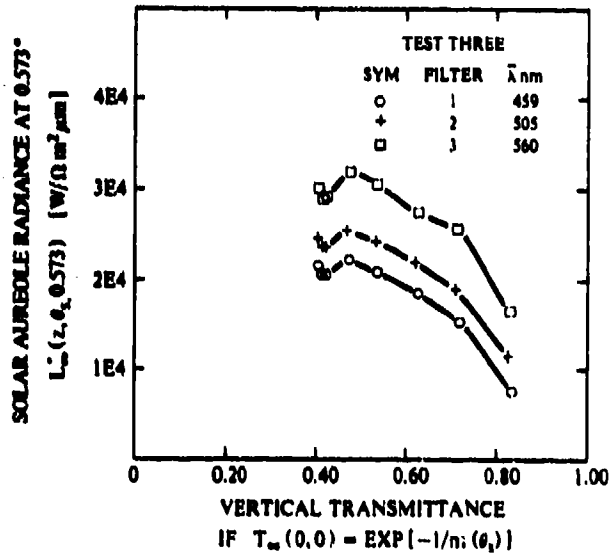

Fig. 3-7. Solar aureole radiance vs vertical transmittance (Eq. 3.26) for 2 September 1964.

Any sky radiance measurement made near the sun without occultation of the sun is questionable and should be tested in some fashion. The above method appears to be a valid testing procedure.

This test can be run for the sky scanner used on 2 September 1964 for various angles from the sun smaller than 55 degrees to establish which scattering angles have valid sky radiance measurements and which contain spurious sun reflections.

3.4 Large Sun Zenith Angle

When the sun zenith angle is relatively large, the solar almucantar contains a large enough range of scattering angles so that Eq. (3.15) can be integrated over 4π thus

$$2\pi \int_0^\infty L^*_\infty(z,\theta_s,\beta)\sin\beta\, d\beta / [\,{}_s e(z)\, m(\theta_s)] - \int_{4\pi} \tau_\infty(z,\beta)\, d\Omega + \int_{4\pi}\int_\infty^z C(z)\, dz\, d\Omega \,. \qquad (3.31)$$

Substituting in Eq. (3.13) we get

$$2\pi \int_0^\infty L^*_\infty(z,\theta_s,\beta)\sin\beta\, d\beta / [\,{}_s e(z)\, m(\theta_s)] - {}_s t_\infty(z) + \int_{4\pi}\int_\infty^z C(z)\, dz\, d\Omega \,. \qquad (3.32)$$

The last term in Eq. (3.32) can be rewritten substituting in Eq. (3.4) for $C(z)$

$$\int_{4\pi}\int_\infty^z C(z)\, dz\, d\Omega = \int_{4\pi}\int_\infty^z \int_{4\pi} [L(z,\theta',\phi')\sigma(z,\beta')/{}_s e(z)]\, d\Omega\, dz\, d\Omega + \int_{4\pi}\int_\infty^z [L_{sa}(z)/{}_s e(z)]\, dz\, d\Omega \,. \qquad (3.33)$$

This integrates to

$$\int_{4\pi}\int_\infty^z C(z)\, dz\, d\Omega = \int_\infty^z \{[e(z) - {}_s e(z)]\, s(z)/{}_s e(z)\}\, dz + \int_\infty^z [m_{sa}(z)/{}_s e(z)]\, dz \,. \qquad (3.34)$$

But the first term in Eq. (3.34) can also be written as

$$\int_\infty^z \{[e(z) - {}_s e(z)]\, s(z)/{}_s e(z)\}\, dz = \int_\infty^z [e(z)\, s(z)/{}_s e(z)]\, dz - {}_s t_\infty(z) \,. \qquad (3.35)$$

Therefore combining Eqs. (3.32), (3.34) and (3.35) we get

$$2\pi \int_0^\infty L^*_\infty(z,\theta_s,\beta)\sin\beta\, d\beta / [\,{}_s e(z)\, m(\theta_s)] - \int_\infty^z [e(z)\, s(z)/{}_s e(z)]\, dz + \int_\infty^z [m_{sa}(z)/{}_s e(z)]\, dz \,. \qquad (3.36)$$

By multiplying both sides by the sun scalar irradiance out of the atmosphere ${}_s e(\infty)$, this can also be written as

$$2\pi \int_0^\infty L^*_\infty(z,\theta_s,\beta)\sin\beta\, d\beta / [T_\infty(z,\theta_s)\, m(\theta_s)] - \int_\infty^z \exp\left[\int_\infty^z \alpha(z)\, dr\right][e(z)\, s(z) + m_{sa}(z)]\, dz \,. \qquad (3.37)$$

No Absorption

When there is no absorption the total scalar irradiance $e(z)$ does not change with altitude, therefore it may be taken out of the integral. Also the attenuation coefficient $\alpha(z)$ is equal to the scattering coefficient $s(z)$. In addition there is no emission thus $m_{sa}(z)$ equals zero. Making these substitutions into Eq. (3.37) and transposing $m(\theta_s)$ we have

$$2\pi \int_0^\infty L^*_\infty(z,\theta_s,\beta)\sin\beta\, d\beta / T_\infty(z,\theta_s) - e(z) \int_\infty^z \exp\left[\int_\infty^z s(z)\, dr\right] s(z)\, m(\theta_s)\, dz \,. \qquad (3.38)$$

For the sun angles where $m(\theta_s)$ equals $sec\theta_s$ and dr equals $sec\theta\, dz$, we now have an integral of the form $e^u du$ where u equals $\int s(z)sec\theta_s dz$ and du equals $s(z)sec\theta_s dz$. Therefore, we need a large sun zenith angle to get full coverage of the scattering angles 0 to 180 degrees but we need the sun zenith angle to be equal to or less than 70 degrees so that the airmass is equal to $sec\theta_s$. These two requirements are a bit contradictory. Assuming the two requirements reasonably compatible at 70 to 80 degrees zenith angle, we can integrate to get

$$2\pi \int_0^\pi L_\infty^\circ(z,\theta_s,\beta)\sin\beta\, d\beta / T_\infty(z,\theta_s) = \epsilon(z)[T_\infty(z,\theta_s)^{-1} - 1] . \quad (3.39)$$

Transposing the transmittance terms and simplifying we have

$$2\pi \int_0^\pi L_\infty^\circ(z,\theta_s,\beta)\sin\beta\, d\beta / [1 - T_\infty(z,\theta_s)] = \epsilon(z) . \quad (3.39)$$

When there is no absorption the normalized equilibrium radiance from Eq. (2.49) is

$$\int_{4\pi} L_\eta(z,\theta,\phi)\, d\Omega = \epsilon(z) . \quad (3.40)$$

Therefore, Eqs. (3.39) and (3.40) imply that for the solar almucantar at relatively large sun zenith angles,

$$L_\eta(z,\theta_s,\beta) = L_\infty^\circ(z,\theta_s,\beta)/[1 - T_\infty(z,\theta_s)] . \quad (3.41)$$

4. VOLUME SCATTERING FUNCTION

4.1 Integrating Nephelometer

The Visibility Laboratory integrating nephelometer was first described in Duntley *et al.* (1970). Measurements were made on the ground and airborne by the Visibility Laboratory with this instrument from 1968 through 1975 in locations in Thailand, the continental United States and in Europe. From 1977 through 1980 similar measurements were made in Europe with a comparable folded path instrument described in Duntley *et al.* (1975).

The integrating nephelometer measures three scattering properties: the total volume scattering coefficient $s(z)$, and the volume scattering function $\sigma(z,\beta)$ at 30 and 150 degrees scattering angle. Measurements between 1968 and 1980 were made with various narrow and broad band spectral sensitivities in the visible spectrum and very near infrared, with mean wavelengths from 478 to 765 nanometers.

When the integrating nephelometer data are put into the form of the ratio to the Rayleigh scattering, some of the differences due to wavelength and air density changes with altitude disappear. Let us define a ratio $Q(z)$ as the ratio of the total volume scattering coefficient to the Rayleigh volume scattering coefficient ${}_R s(z)$.

$$Q(z) = s(z)/{}_R s(z) . \quad (4.1)$$

Similarly let us define a ratio $\mathcal{Q}(z,\beta)$ as the ratio of the total volume scattering function to the Rayleigh volume scattering function ${}_R\sigma(z,\beta)$

$$\mathcal{Q}(z,\beta) = \sigma(z,\beta)/{}_R\sigma(z,\beta) . \quad (4.2)$$

When the scattering function ratio $\mathcal{Q}(z,\beta)$ is graphed as a function of the total scattering coefficient ratio $Q(z)$, a single function results for each scattering angle β, regardless of the filter, or whether the data are ground level as in Fig. 4-1 or airborne as in Fig. 4-2. All the integrating nephelometer data from 1968 through 1980 are similar regardless of location of measurement or filter.

The superimposed curves are from the catalog of normalized volume scattering functions from Barteneva (1960).

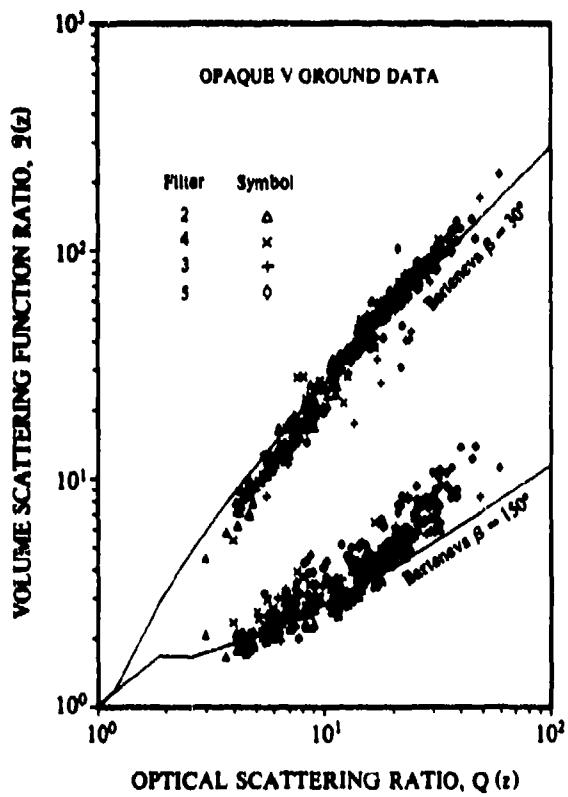

Fig. 4-1. Comparison of multi-spectral volume scattering function ratios measured by Visibility Laboratory ground-based nephelometer with the photopic ratios from Barteneva (1960).

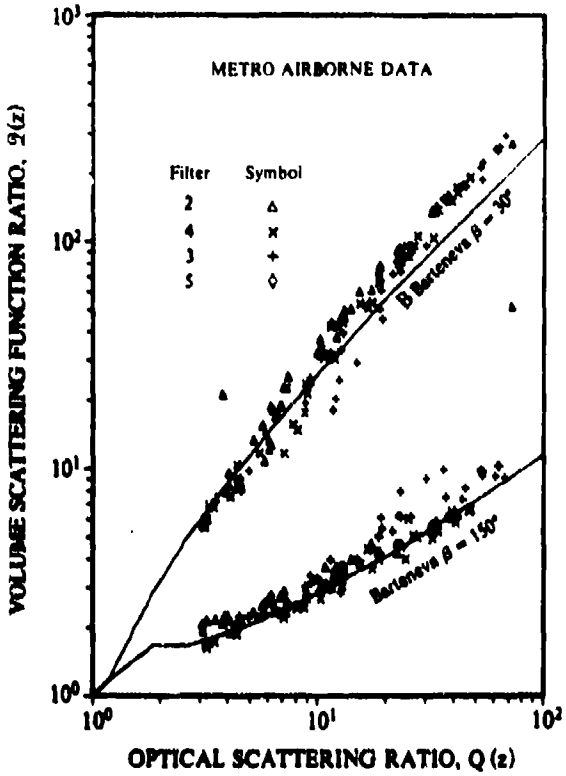

Fig. 4-2. Comparison of multi-spectral volume scattering function ratios measured by Visibility Laboratory airborne nephelometer with the photopic ratios from Barteneva (1960).

4.2 Barteneva Catalog

Barteneva (1960) provided a catalog of normalized directional scattering functions $\sigma(\beta)/s$ for the photopic sensor based upon 624 measurements made with a nephelometer during 1955 through 1958 in various locations in the USSR and at sea. For each volume scattering function she gives a range of total volume scattering coefficient appropriate to that function.

The range of total volume scattering coefficients is from Rayleigh to heavy fog, for ground level. Her catalog of gradual functions, classes 1 through 10, are appropriate for very clear to heavy haze, but not fog. This range of functions is applicable to the troposphere under conditions appropriate for flying using visual flight rules. This also describes the conditions under which the aircraft flew during the Visibility Laboratory data missions. Since the ground-based data were taken in conjunction with the flights, these same conditions are also appropriate for the ground-based data.

The Barteneva catalog was first interpreted in terms of the median total volume scattering value for each scattering function class. Then the ratio Q was computed for these median s values. Similarly, the value of the median volume scattering function $\sigma(0,\beta)$ for 30 and 150 degrees was computed by multiplying the normalized functions by the median s values. Then the ratio to Rayleigh $\Sigma(z,\beta)$ was computed and the curves in Figs. 4-1 and 4-2 graphed for the Barteneva data.

All the Visibility Laboratory nephelometer data for total volume scattering and the scattering functions at 30 and 150 degrees agree with the Barteneva catalog of gradual functions. Thus it has been assumed that the Barteneva catalog is appropriate for specifying the directional scattering for all the scattering angles 0 to 180 degrees for various sensors in the visible spectrum in the troposphere.

The further step of representing the catalog by equations has been made by Johnson and Hering (1981a). A full analytic representation in the form of Henyey-Greenstein functions is presented in Hering (1981b).

Graphs of the normalized volume scattering functions as a function of scattering angle for the Barteneva catalog are given in Fig. 4-3 for the gradual classes and Fig. 4-4 for the steeper classes.

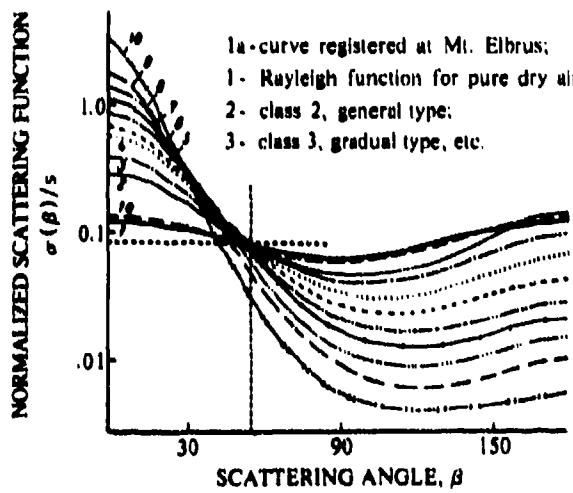

Fig. 4-3. Normalized volume scattering function for gradual classes from Fig. 1 Barteneva (1960).

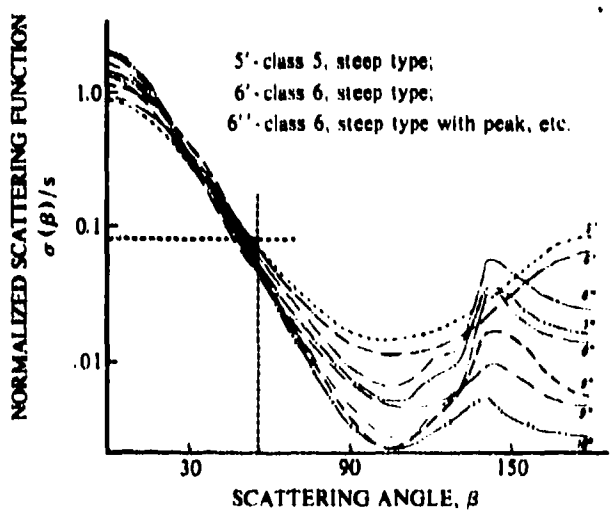

Fig. 4-4. Normalized volume scattering function for steeper classes from Fig. 2 Barteneva (1960).

4.3 Average Volume Scattering Function at 55°

The average normalized volume scattering function is

$$\int_{4\pi} [\sigma(\beta)/s]d\Omega / \int_{4\pi} d\Omega = 1/(4\pi) = .08 . \qquad (4.3)$$

The Rayleigh normalized volume scattering function can be computed from the approximation

$${}_R\sigma(\beta)/{}_Rs = 3(1+\cos^2\beta)/(16\pi) . \qquad (4.4)$$

Equations (4.3) and (4.4) were combined and the ensuing equation solved to obtain the scattering angle at which the Rayleigh normalized volume scattering function is equal to the average value of $1/4\pi$. It was found to be 55 degrees

$${}_R\sigma(55)/{}_Rs = 1/(4\pi) . \qquad (4.5)$$

The graphs in Figs. 4-3 and 4-4 are marked at scattering angle 55 degrees and at the normalized volume scattering function equal to 0.08. From these graphs we see that the scattering angle of 55 degrees yields a reasonable approximation of the average volume scattering function for all the scattering functions except the gradual classes 9 and 10, that is,

$$\sigma(55)/s = 1/(4\pi) . \qquad (4.6)$$

In reviewing the graphs of measured nephelometer data, it is noted that none of the total scattering coefficient ratios $Q(z)$ exceeded 100. That is, gradual classes 1 through 8 [Q(8) = 114] were encountered but never 9 or 10 [Q(9) = 201 and Q(10) = 237]. Therefore for modeling the atmospheres measured from 1968 through 1981 in the visible spectrum, it is reasonable to use Eq. (4.6) as part of the model assumptions.

4.4 Method of Obtaining Single Scattering Albedo from Horizon Sky

Roessler and Faxvog (1981) developed equations for the horizon sky luminance as a function of the single scattering albedo after assuming both an isotropic scattering function and an isotropic luminance distribution. The technique can be made more generally applicable by developing the equations for the horizon at a scattering angle of 55 degrees from the sun.

Horizon Sky at 55° from Sun

The equation for the path function at 55 degrees scattering angle can be expressed as a function of the sun component separate from the sky-terrain component in a manner similar to Eq. (3.2)

$$L_*(z,\theta,55\,\beta) = {}_s\epsilon(z)\sigma(z,55) + \int_{4\pi} L(z,\theta',\phi')\sigma(z,\beta')d\Omega + L_{*_a}(z) . \qquad (4.7)$$

Substituting Eq. (4.6) into Eq. (4.7) and assuming the sky-terrain or diffuse scalar irradiance ${}_d\epsilon(z)$ is isotropic we get

$$L_*(z,\theta,55\,\beta) = {}_s\epsilon(z)s(z)/(4\pi) + {}_d\epsilon(z)s(z)/(4\pi) + L_{*_a}(z) . \qquad (4.8)$$

Since the total scalar irradiance is the sun plus the sky-terrain scalar irradiance, Eq. (4.8) can be written as

$$L_*(z,\theta,55\,\beta) = \epsilon(z)s(z)/(4\pi) + L_{*_a}(z) . \qquad (4.9)$$

Dividing both sides by the attenuation coefficient and expressing the emitted path function according to Eq. (2.7) we get an equation for the equilibrium radiance

$$L_q(z,\theta,55\,\beta) = \epsilon(z)s(z)/[\alpha(z)4\pi] + a(z)L(\lambda,T)/\alpha(z) . \qquad (4.10)$$

This can be expressed in terms of the single scattering albedo ω (from Eq. (2.39)) as

$$L_q(z,\theta,55\,\beta) = \omega(z)\epsilon(z)/(4\pi) + [1-\omega(z)]L(\lambda,T) . \qquad (4.11)$$

The general equation for the horizon sky radiance at 55 degrees scattering angle from Eq. (2.57) is

$$L^*_\infty(z,90,55\,\beta) = L_q(z,90,55\,\beta)[1-T_\infty(z,90)] . \qquad (4.12)$$

Therefore from Eq. (4.11) the horizon sky radiance at 55 degrees is

$$L^*_\infty(z,90,55\,\beta) = \{\omega(z)\epsilon(z)/(4\pi) + [1-\omega(z)]L(\lambda,T)\}[1-T_\infty(z,90)] . \qquad (4.13)$$

The above equation assumes that the attenuation coefficient is horizontally isotropic and therefore the horizon sky must be cloud free.

Visible Spectrum

In the visible spectrum $L(\lambda,T)$ is negligible. Also for the photopic at sea level $T_\infty(0,90)$ is negligible and Eq. (4.13) becomes

$$L_\infty^\circ(0,90,55\beta) = \omega(0)e(0)/4\pi . \quad (4.14)$$

Thus the single scattering albedo ω can be determined by measuring the horizon sky at 55 degrees and the total scalar irradiance at sea level

$$\omega(0) = L_\infty^\circ(0,90,55\beta)4\pi/e(0) . \quad (4.15)$$

Since this is an approximative method, the precision level of the resultant $\omega(0)$ is not expected to be high. However, it can still be quite useful as one measure of the single scattering albedo.

When there is no absorption $\omega = 1$ and the horizon sky should equal the average scalar irradiance $e(0)/(4\pi)$

$$L_\infty^\circ(0,90,55\beta) = e(0)/(4\pi) . \quad (4.16)$$

4.5 Method of Obtaining Scattering Transmittance from Sky Radiance Ratios at 55 Degrees

When absorption is negligible, the general equation for the equilibrium radiance at 55 degrees scattering angle Eq. (4.11) reduces to

$$L_q(z,\theta,55\beta) = e(z)/4\pi . \quad (4.17)$$

Also when absorption is negligible the total scalar irradiance $e(z)$ is constant with altitude, therefore the equilibrium radiance at 55 degrees is also constant with altitude. Rearranging the equilibrium radiance form of the equation of transfer Eq. (2.17) we get

$$[L(z,\theta,55\beta) - L_q(z,\theta,55\beta)]^{-1}\, dL(z,\theta,55\beta) = -s(z)dr , \quad (4.18)$$

where the total scattering coefficient $s(z)$ has been substituted for the attenuation coefficient since absorption is negligible. Since the equilibrium radiance is a constant Eq. (4.18) can be integrated with respect to altitude

$$\int_{L_0}^{L_f} [L(z,\theta,55\beta) - L_q(z,\theta,55\beta)]^{-1}\, dL(z,\theta,55\beta) = -\int_0^r s(z)dr . \quad (4.19)$$

The result of the integration is

$$L_r(z,\theta,55\beta) = L_0(z_f,\theta,55\beta)\, {}_sT_r(z,\vartheta) + L_q(z,\theta,55\beta)[1 - {}_sT_r(z,0)] \quad (4.20)$$

where ${}_sT_r(z,\theta)$ is the transmittance due to scattering.

Sky Radiance Ratio at 55°

For sky radiance at 55 degrees scattering angle, the inherent radiance L_0 is equal to zero and Eq. (4.20) becomes

$$L_\infty^\circ(z,\theta,55\beta) = L_q(z,\theta,55\beta)[1 - {}_sT_\infty(z,\theta)] . \quad (4.21)$$

Now when 55 degree sky radiances at two zenith angles θ and θ' are ratioed, since the equilibrium radiance is equivalent, the sky radiance ratio is solely a function of the scattering transmittance

$$L_\infty^\circ(z,\theta,55\beta)/L_\infty^\circ(z,\theta',55\beta) = [1 - {}_sT_\infty(z,0)^{m(\theta)}] / [1 - {}_sT_\infty(z,0)^{m(\theta')}] . \quad (4.22)$$

Although Eq. (4.22) cannot be solved for directly, it can be solved by iterative means. Error analysis indicates that the zenith angle difference $\theta - \theta'$ should be large to minimize the error in the resultant vertical transmittance ${}_sT_\infty(z,0)$.

Visible Spectrum

In the visible spectrum, absorption is negligible except for ozone. The total transmittance in the visible spectrum would thus be approximated by the product of the scattering transmittance times the ozone transmittance

$$T_\infty(z,0) = {}_sT_\infty(z,0)\, {}_oT_\infty(z,0) . \quad (4.23)$$

To illustrate the use of Eqs. (4.22) and (4.23), we again refer to the sky radiance and solar transmissometer data taken on the Visibility Laboratory rooftop in 1964. The atmosphere on 2 September 1964 was optically stable during the afternoon as illustrated in Section 3.3. Thus evaluation of the scattering transmittances throughout the afternoon should give us an estimate of the precision of the estimation method for broad band sensors in the visible. Equation (4.22) was evaluated for all sky radiances at 55 degrees plus or minus 2.5 degrees scattering angle for θ from 81.6 to 64.7 degrees and θ' from 64.7 to 2.8 degrees. Later error analyses indicated that some of these zenith angle combinations are less error prone than others. Hence, the averages in Table 4.1 are less accurate than can be obtained with a smaller yet better selection of zenith angle combinations. However, they are presented herein as a first approximation.

The transmittance ratios in Table 4.1 are the transmittances based on Eq. (4.22) times the ozone transmittance divided by the transmittance from the solar transmissometer. The ozone transmittance is noted at the bottom of each column. The transmittance comparison is best for Filter 1 which is a relatively narrow band filter with the least absorption. The near noon data compare

Table 4.1. Comparison of transmittance determination procedures (sky radiance ratio method vs solar transmissometer).

Nominal Sun Zenith Angle θ_s (degrees)	TOTAL TRANSMITTANCE RATIO (From Eq (4.22, and 4.23) and Solar Transmissometer Measurements)			
	Filter 1 $\bar{\lambda}$ = 459 nm	Filter 2 $\bar{\lambda}$ = 505 nm	Filter 3 $\bar{\lambda}$ = 560 nm	Filter 4 $\bar{\lambda}$ = 661 nm
24	.954	.891	.894	.900
30	.944	.893	.894	.905
40	1.045	1.011	1.039	1.038
50	1.045	1.013	1.041	1.047
60	1.034	1.006	1.031	1.044
70	1.030	1.014	1.042	1.050
80	1.002	.998	1.031	1.045
Average	1.008	.975	.995	1.004
Standard Deviation	.043	.057	.069	.070
Ozone Contribution ${}_{o}T_{\infty}$ (0,0)	.996	.984	.969	.978

least well. The accuracy is probably sufficient to warrant further development of the method to improve the precision level.

Use of sky radiances at 55 degrees scattering angle should be an improvement on the sky ratio method described in Duntley *et al.* (1972) Section 2.1 and in Duntley *et al.* (1978) Section 2.2. That method, which stemmed from the nomographic method of Kushpil' and Petrova (1971), used sky radiances at all scattering angles. Kushpil' and Petrova (1971) suggested use of ratios at 57.2 degrees scattering angle for the visible spectrum and 53.9 degrees for the near infrared portion of the spectrum but did not give a theoretical basis for the nomograph or for the selection of these angles.

4.6 Method of Obtaining Aerosol Optical Thickness from Solar Almucantar

The basic equation for the sky radiance in the solar almucantar Eq. (3.15) can be rewritten expressing the optical thickness function in two components, the Rayleigh or molecular ${}_{R}\tau_{\infty}(z,\beta)$ and the Mie ${}_{M}\tau_{\infty}(z,\beta)$

$$L^{*}_{\infty}(z,\theta_s,\beta) / [{}_{s}a(z)m(\theta_s)] = {}_{R}\tau_{\infty}(z,\beta) + {}_{M}\tau_{\infty}(z,\beta) + \int_{\infty}^{z} C(z)dz \,. \qquad (4.24)$$

For simplicity the left hand ratio is defined as a function $\mu(z,\beta)$

$$\mu(z,\beta) = L^{*}_{\infty}(z,\theta_s,\beta) / [{}_{s}a(z)m(\theta_s)] \,. \qquad (4.25)$$

If we have in the almucantar a large enough range of scattering angles, both sides of Eq. (4.24) can be integrated over 4π and Eq. (3.13) substituted in to obtain

$$2\pi \int_{0}^{\pi} \mu(z,\beta) \sin\beta \, d\beta = {}_{R}t_{\infty}(z) + {}_{M}t_{\infty}(z) + 2\pi \int_{0}^{\pi} \int_{\infty}^{z} C(z)dz \sin\beta \, d\beta \,. \qquad (4.26)$$

where ${}_{R}t_{\infty}(z)$ is the Rayleigh optical thickness and ${}_{M}t_{\infty}(z)$ is the Mie optical thickness. The last term in both Eqs. (4.24) and (4.26) is the diffuse component due to the contribution of the relatively non-directional sky, apparent terrain radiance and emission. All the equations up to this point are not approximations and hold for an atmosphere with or without absorption and/or emission. Thus, they are equally as valid in the infrared.

Livshits and Pavlov (1970) make the assumption that in the photopic or visible portion of the spectrum, the sky luminance or radiance in the almucantar for scattering angles 90 to 180 degrees is essentially a function of the Rayleigh optical thickness function and the diffuse component, and that the diffuse component is the same for 0 to 90 degrees as it is for 90 to 180 degrees scattering angle. This assumes homogeneity in the almucantar and thus is limited to cloudless skies. Thus since the Rayleigh scattering is symmetrical about 90 degrees

$$2[2\pi \int_{\pi/2}^{\pi} \mu(z,\beta) \sin\beta \, d\beta]$$

$$= {}_R t_\infty(z) + 2\pi \int_0^{\pi} \int_z^{\infty} C(z) dz \sin\beta \, d\beta \, . \qquad (4.27)$$

Also it follows that the Mie optical thickness is the integral of the forward portion of the function less the integral of the back portion

$${}_M t_\infty(z) = 2\pi \int_0^{\pi/2} \mu(z,\beta) \sin\beta \, d\beta$$

$$- 2\pi \int_{\pi/2}^{\pi} \mu(z,\beta) \sin\beta \, d\beta \, . \qquad (4.28)$$

Livshits and Pavlov (1970) also obtained the total optical thickness $t_\infty(z)$ from

$$t_\infty(z) = {}_R t_\infty(z) + {}_M t_\infty(z) + {}_a t_\infty(z) \, . \qquad (4.29)$$

where ${}_a t_\infty(z)$ is the optical thickness due to absorption. They obtain the Rayleigh thickness theoretically, and assume the absorption is primarily due to ozone in the visible wavelengths. Ozone absorption was assumed to be the yearly average value for a given wavelength. They got good comparison to total optical thickness values obtained with the Langley or Bouger method for short wavelengths where there are no other absorption bands. They did not compare as well at the longer wavelengths. We suspect absorption other than for ozone in the longer wavelengths in the visible rather than an error in the aerosol optical thickness.

Scattering Angle 55°

The disadvantage of Eq. (4.28) is the need for a large sun zenith angle so that a large range of scattering angles are available in the solar almucantar radiances.

Since the ratio of the volume scattering function at 55 degrees to the scattering coefficient is $1/(4\pi)$ for the Rayleigh and the total scattering (Eqs. (4.5) and (4.6)), it must also be $1/(4\pi)$ for Mie scattering as well

$${}_R\sigma(z,55)/{}_R s(z) = \sigma(z,55)/s(z)$$

$$= {}_M\sigma(z,55)/{}_M s(z) = 1/(4\pi) \, . \qquad (4.30)$$

Thus the ratio of the optical thickness function at 55 degrees to the optical thickness must also be $1/(4\pi)$ for each component as well as the total scattering

$${}_R\tau_\infty(z,55)/{}_R t_\infty(z) = \tau_\infty(z,55)/{}_s t_\infty(z)$$

$$= {}_M\tau_\infty(z,55)/{}_M t_\infty(z) = 1/(4\pi) \, . \qquad (4.31)$$

Now we can express the Mie optical thickness function in terms of the Mie optical thickness by rearranging Eq. (4.31)

$${}_M\tau_\infty(z,55) = {}_M t_\infty(z)/(4\pi) \, . \qquad (4.32)$$

Using the same rationale as Livshits and Pavlov (1970), that the angles 90 to 180 degrees in scattering angle describe the diffuse and Rayleigh components for the angles 0 to 90 degrees, we can say that

$$\mu(z,180-55) = {}_R\tau_\infty(z,55) + \int_z^{\infty} C(z) dz \, . \qquad (4.33)$$

Also from Eq. (4.24) we have

$$\mu(z,55) = {}_M\tau_\infty(z,55) + {}_R\tau_\infty(z,55) + \int_z^{\infty} C(z) dz \, . \qquad (4.34)$$

Subtracting Eq. (4.33) from Eq. (4.34) we get

$${}_M\tau_\infty(z,55) = \mu(z,55) - \mu(z,125) \, . \qquad (4.35)$$

Now combining with Eq. (4.32) we get

$${}_M t_\infty(z) = 4\pi[\mu(z,55) - \mu(z,125)] \, . \qquad (4.36)$$

The solar almucantar contains both 55 and 125 degrees scattering angle for sun zenith angles 62.5 to 90 degrees. Thus for these solar zenith angles a measurement of the scalar sun irradiance and sky radiances in the solar almucantar at 55 and 125 degrees from the sun would yield a measure of the Mie optical thickness through the atmosphere. As long as the sky radiance distribution shows brighter areas 0 to 90 degrees than 90 to 180 degrees, this scheme will work. Equation (4.36) also is valid when atmospheric emission is present as long as the emission does not swamp out the directional scattering effects.

Alternate Expression

An alternate expression for obtaining the aerosol optical thickness from sky radiances when no sun scalar irradiance measurement is available can be developed. Substituting Eq. (4.25) into Eq. (4.36) and rearranging we get

$${}_M t_\infty(z) = 4\pi[L_\infty^*(z,\theta_s,55\,\beta)$$

$$- L_\infty^*(z,\theta_s,125\beta)] / [{}_s\epsilon(z) m(\theta_s)] \, . \qquad (4.37)$$

The sun scalar irradiance can be obtained from the average sun irradiance out-of-the atmosphere ${}_s\bar{\epsilon}(\infty)$ by

$$ {}_s\epsilon(z) = {}_s\bar{\epsilon}(\infty)\, T_\infty(z,0)^{m(\theta_s)}\, (\Psi/\bar{\Psi})^2 , \qquad (4.38) $$

where Ψ is the angular solar diameter for that date and $\bar{\Psi}$ the average angular solar diameter. Also the total transmittance can be expressed as a function of the component optical thicknesses from Eq. (4.29)

$$ T_\infty(z,0) = \exp\left[-{}_R t_\infty(z) - {}_M t_\infty(z) - {}_a t_\infty(z) \right] . \qquad (4.39) $$

Substituting Eqs. (4.38) and (4.39) into Eq. (4.37) and rearranging we get

$$ {}_M t_\infty(z) \exp\left[-{}_M t_\infty(z) m(\theta_s) \right] $$

$$ = 4\pi \left[L^*_\omega(z,\theta_s,55\,\beta) - L^*_\omega(z,\theta_s,125\beta) \right] $$

$$ / \left[{}_s\bar{\epsilon}(\infty) m(\theta_s) (\Psi/\bar{\Psi})^2 \exp\left\{ -m(\theta_s) \left[{}_R t_\infty(z) + {}_a t_\infty(z) \right] \right\} \right] . \qquad (4.40) $$

Equation (4.40) cannot be solved directly for the aerosol optical thickness but by interative means it is readily obtained. It assumes a reasonable estimate of absorption optical thickness can be made such as assuming only ozone absorption in the visible or that a value can be obtained through use of Program LOWTRAN at other wavelengths.

Validation Studies

The two methods of obtaining the total optical thickness and hence transmittance from solar almucantar sky radiances at 55 and 125 degrees using Eqs. (4.37) and (4.40) with Eq. (4.29) were tested using the 1964 Visibility Laboratory rooftop data previously described in Section 3.3.

The scanner radiance grid included almucantar measurements within ±0.7 degrees for all four filters for the 2 September 1964 nominal 70 degrees sun zenith angle data packages. The solar transmissometer value of transmittance was used in Eq. (4.38) to obtain the value of scalar sun irradiance ${}_s\epsilon(z)$ for use in Eq. (4.37). The values of and basis for the scalar sun irradiance out of the atmosphere ${}_s\bar{\epsilon}(\infty)$, the Rayleigh optical thickness and ozone optical thickness are given in Appendix A.

The total optical thickness $t_\infty(0)$ and total transmittance $T_\infty(0,0)$ from the solar transmissometer are given for each filter in Table 4.2. The ratio of the optical thickness derived using Eq. (4.37) to the solar transmissometer value is given in column 4, and the ratio for Eq. (4.40) in column 5. Similarly, the ratio of the derived transmittances to measured values are given in columns 7 and 8 respectively. The values compare well for the first 3 filters and less well for filter 4 meanwavelength 661 nanometers, although even there the transmittances are within 2 percent. Livshits and Pavlov (1970) similarly found closer comparisons at the shorter wavelengths for monochromatic measurements.

Thus the shorter method, using the almucantar at 55 and 125 degrees with or without an independent sun irradiance measurement, appears to be valid for narrow band and broad band sensors in the visible spectrum.

The alternate equation Eq. (4.40) is particularly useful with airborne scanner data where independent measurements of sun irradiance are not available. This method was used to obtain the aerosol optical thickness for flight C-466 airborne data at 6 and 0.2 kilometers for use in the example in Section 2.4 Tables 2.5 and 2.6.

Since this is an approximative method, the resultant aerosol optical thickness precision may not be high, but the resultant transmittances have high precision as can be seen in Table 4.2. The method requires an unobscured sun and cloud-free sky at 55 and 125 degrees from the sun in the almucantar.

5. SUMMARY

Some implications of the equation of transfer as it relates to a scattering and absorbing medium have been explored. The major implication is that a measurement of the 4π radiance distribution can yield a great deal of information about the atmosphere both in the visible and the near infrared. If the solar almucantar is cloud-free the

Table 4.2. Comparison of transmittance determination procedures (solar alumcantar radiances vs solar transmissometer).

Filter Number	Mean Wavelength $\bar{\lambda}$ nm	TOTAL OPTICAL THICKNESS $t_\infty(z)$			TOTAL TRANSMITTANCE $T_\infty(0,0)$		
		Transmissometer Measurement	"Derived to Meas." Ratios		Transmissometer Measurement	"Derived to Meas." Ratios	
			Using Eq. (4.37)	Using Eq. (4.40)		Using Eq. (4.37)	Using Eq. (4.40)
1	459	.296	.96	.95	.743	1.01	1.01
2	505	.241	1.02	1.03	.786	99	.99
3	560	.200	.95	1.02	.819	1.01	1.00
4	661	.143	.86	.84	.867	1 02	1.02

aerosol optical thickness can be derived. If the 4π radiance distribution is measured at several altitudes, the radiance arrays can be tested for consistency and, if consistent, a measure of absorption obtained. The Visibility Laboratory data catalog of radiances, both airborne and ground-based are a mine of information waiting to be tapped. This catalog is useful for testing methods of retrieval of basic scattering and absorption information about the atmosphere as well as for development of atmospheric models.

6. ACKNOWLEDGEMENTS

This report has been prepared for the Air Force Geophysics Laboratory under Contract No. F19628-82-C-0060. The author wishes to thank Richard W. Johnson for his encouragement and help in developing the conceptual material for this report. In addition the author wishes to thank the members of the Visibility Laboratory technical staff for their assistance in preparing this report and in particular to acknowledge the contributions of Ms. Alicia G. Hill and Mr. John C. Brown our specialists in computer assisted document preparation.

7. REFERENCES

Barteneva, O. D., "Scattering Functions of Light in the Atmospheric Boundary Layer", Bull. Acad. Sci. U.S.S.R., Geophysics Series, 1237-1244 (1960).

Brown, D. R. I., *Natural Illumination Charts*, Report 374-1, Project Ns-714-100, Department of the Navy, Bureau of Ships, Washington, D.C. (1952).

Chandrasekhar, S., *Radiative Transfer*, (Dover Pub. Inc., New York, 1960).

Driscoll, W. G. and W. Vaughan, *Handbook of Optics*, (McGraw-Hill Book Co., New York, 1978).

Duntley, S. Q., A. R. Boileau, and R. W. Preisendorfer, "Image Transmission by the Troposphere I", J. Opt. Soc. Am. 47, 499-506 (1957).

Duntley, S. Q., "Directional Reflectance of Atmospheric Paths of Sight", University of California, San Diego, Scripps Institution of Oceanography, Visibility Laboratory, Report No. 69-1, AD #688265 (1969).

Duntley, S. Q., R. W. Johnson, J. I. Gordon, and A. R. Boileau, "Airborne Measurements of Optical Atmospheric Properties at Night", University of California, San Diego, Scripps Institution of Oceanography, Visibility Laboratory, SIO Ref. 70-7, AFCRL-70-0137, NTIS No. AD 870 734 (1970).

Duntley, S. Q., R. W. Johnson, and J. I. Gordon, "Airborne Measurements of Optical Atmospheric Properties, Summary and Review", University of California, San Diego, Scripps Institution of Oceanography, Visibility Laboratory, SIO Ref. 72-82, AFCRL-72-0593, NTIS No. AD 754 898 (1972).

Duntley, S. Q., R. W. Johnson, and J. I. Gordon, "Airborne Measurements of Optical Atmospheric Properties, Summary and Review II", University of California, San Diego, Scripps Institution of Oceanography, Visibility Laboratory, SIO Ref. 75-26, AFCRL-TR-75-0457, NTIS No. ADA 022 675 (1975).

Duntley, S. Q., R. W. Johnson and J. I. Gordon, "Airborne Measurements of Optical Atmospheric Properties in Northern Germany", University of California, San Diego, Scripps Institution of Oceanography, Visibility Laboratory, SIO Ref. 76-17, AFGL-TR-76-0188, NTIS No. ADA 035 571 (1976).

Duntley, S. Q., R. W. Johnson and J. I. Gordon, "Airborne Measurements of Optical Atmospheric Properties, Summary and Review III", University of California, San Diego, Scripps Institution of Oceanography, Visibility Laboratory, SIO Ref. 79-5, AFGL-TR-78-0286, NTIS No. ADA 073 121 (1978).

Edlen, B., "Dispersion of Standard Air", J. Opt. Soc. Am. 43, 339 (1953).

Fenn, R. W., "OPAQUE - A Measurement Program on Optical Atmospheric Quantities in Europe, Vol. I The NATO OPAQUE Program", Special Reports No. 211, AFGL-TR-78-0011 (1978).

Gast, P. R., A. S. Jursa, J. Castelli, S. Basu, and J. Aarons, "Solar Electromagnetic Radiation", Chapter 16 in *Handbook of Geophysics and Space Environments*, S. L. Valley AFCRL, Ed. (McGraw-Hill Book Co., New York 1965), p. 16-7.

Hering, W. S., "An Assessment of Operational Techniques for Estimating Visible Spectrum Contrast Transmittance", in *SPIE Proceedings on Atmospheric Effects on Electro-Optical, Infrared and Millimeter Wave System Performance*, Vol. 305, pp. 119-124 (1981a).

Hering, W.S., "An Operational Technique for Estimating Visible Spectrum Contrast Transmittance", University of California, San Diego, Scripps Institution of Oceanography, Visibility Laboratory, SIO Ref. 82-1, AFGL-TR-81-0198 (1981b).

Inn, E. C. Y. and Y. Tanaka, "Ozone Absorption", J. Opt. Soc. Am. 43, 872 (1953).

Johnson, F. R., "The Solar Constant", J. Meteoro. 11, 431-439 (1954).

Johnson, R. W., W. S. Hering, J. I. Gordon, B. W. Fitch and J. E. Shields, "Preliminary Analysis and Modelling Based Upon Project OPAQUE Profile and Surface Data", University of California, San Diego, Scripps Institution of Oceanography, Visibility Laboratory, SIO Ref. 80-5, AFGL-TR-79-0285, NTIS No. ADB 052 172L (1979).

Johnson, R. W. and J. I. Gordon, "Airborne Measurements of Atmospheric Volume Scattering Coefficients in Northern Europe, Summer 1978", University of California, San Diego, Scripps Institution of Oceanography, Visibility Laboratory, SIO Ref. 80-20, AFGL-TR-80-0207, NTIS No. ADA 097 134 (1980).

Johnson, R. W. and W. S. Hering, "Measurements of Optical Atmospheric Quantities in Europe and their Application to Modelling Visible Spectrum Contrast Transmittance", *NATO/AGARD-CP-300 Proceedings on Special Topics in Optical Propagation*, pp. 14-1 to 14-12 (1981a).

Johnson, R. W. and W. S. Hering, "An Analysis of Natural Variations in European Sky and Terrain Radiance Measurements", University of California, San Diego, Scripps Institution of Oceanography, Visibility Laboratory, SIO Ref. 82-6, AFGL-TR-81-0317, NTIS No. ADA 120 487 (1981b).

Kasten, F., "A New Table and Approximation Formula for the Relative Optical Air Mass", Arch., Met. Geophys. Bioklim. **B14**, 206-233 (1965).

Kushpil', V. I. and L. F. Petrova, "Determination of the Atmospheric Transmittance from Sky Brightness Distribution", Optical Technology **38**, No. 4, 191-193 (1971).

Livshits, G. Sh. and V. E. Pavlov, "Atmospheric Transmittance and the Interrelationships of Certain Optical Parameters", in *Atmospheric Optics*, Nikolai B. Divari, Ed., translated by S. B. Dresner, Consultants Bureau, New York, (Plenum Publishing Corp., New York, 1970), p. 53-56.

Minnaert, M., "The Photosphere", Chapter 3 in *The Sun*, G. P. Kuiper, Ed., (University of Chicago Press, 1953).

Penndorf, R., "Tables of the Refractive Index for Standard Air and the Rayleigh Scattering Coefficient for the Spectral Region Between 0.2 and 20.0 and Their Application to Atmospheric Optics", J. Opt. Soc. Am. **47**, 176-182 (1957).

Preisendorfer, R. W., *Hydrological Optics, Vols. I and II* (U. S. Department of Commerce, NOAA, ERL, Honolulu, Hawaii 1976).

Pyaskovskaya-Fesenkova, E. V., "Determining the Transmission Coefficient and Degree of Optical Stability of the Earth's Atmosphere", in *Atmospheric Optics*, Nikolai B. Divari, Ed., translated by S. B. Dresner, Consultants Bureau, (Plenum Publishing Corp., New York 1979), p. 151-156.

Roessler, D. M. and F. R. Faxvog, "Visibility in Absorbing Aerosols", Atmospheric Environment **15**, 151-155 (1981).

Tashenov, B. T., "Spectrophotometric Studies of Atmospheric Transmittance and Stability", in *Atmospheric Optics*, Nikolai B. Divari, Ed., translated by S. B. Dresner, Consultants Bureau, (Plenum Publishing Corp., New York, 1970), p. 70-79.

Tyler, J. E. and R. W. Preisendorfer, "Light", Chapter 8 in *The Sea*, M. N. Hill, Ed., (Interscience Publishers, Inc., New York, 1962), Vol. 1, pp. 397-451.

U. S. Standard Atmosphere Supplements (Superintendent of Documents, U. S. Government Printing Office, Washington, D. C., 1966).

U. S. Standard Atmosphere (Superintendent of Documents, U. S. Government Printing Office, Washington, D. C., 1976).

Vigroux, E., "Etude Experimentale de L'Absorption de l'Ozone", Annales de Physic (Paris) (12) **8**, 742-743, 747.

Wolfe, W. L., "Radiation Theory", in *The Infrared Handbook*, W. L. Wolfe and G. J. Zissis, Eds., (U. S. Government Printing Office, Washington, D. C., 1978).

OPTICAL AND RADIOMETRIC CHARACTERISTICS OF SELECTED BROAD BAND SENSORS

The broad band sensors referred to in the text are multipier phototubes with spectral filters interposed between the sensor and the optical signal. The combination of the sensor sensitivity S_λ and the filter transmittance T_λ is the resultant sensitivity of the filtered phototube $S_\lambda T_\lambda$. The standard responses which each optical system attempts to duplicate are indicated as $\overline{S_\lambda T_\lambda}$. These relative spectral response values are normalized to the peak value.

AVIZ Filters

The relative spectral response values for the AVIZ Filters 2 through 6 are graphed in Fig. A-1 and given in tabular form in Table A.1. Filter code 9 is the true photopic response; it is included in Table A.1 for comparative purposes only. The AVIZ filters are applicable to airborne and ground-based data measured by the atmospheric visibility branch of the Visibility Laboratory between 1970 and 1978. The multiplier phototubes used had an S-20 spectral response.

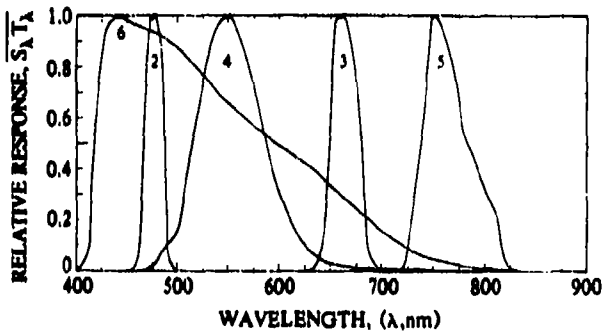

Fig. A-1. Standard spectral responses for AVIZ filters. Peak Wavelengths are: 2 = 475nm Blue, 3 = 660nm Red, 4 = 550nm Photopic, 5 = 750nm N.I.R., 6 = 440nm S-20.

Spectral Characteristics

A summary of the response characteristics of the AVIZ filters is given in Table A.2. The mean wavelength $\bar{\lambda}$ is defined by

$$\bar{\lambda} = \sum_{400}^{1100} \lambda \ \overline{S_\lambda T_\lambda} \ \Delta\lambda \ / \ \delta\lambda \ . \qquad (A.1)$$

The effective passband $\delta\lambda$ is defined by

$$\delta\lambda = \sum_{400}^{1100} \overline{S_\lambda T_\lambda} \ \Delta\lambda \ . \qquad (A.2)$$

The radiometric units for irradiance of $W/m^2\mu m$ are obtained from units of W/m^2 by dividing by the effective passband $\delta\lambda$. Similarly the radiometric units for radiance of $W/sr\,m^2\mu m$ are obtained from units of $W/sr\,m^2$ by dividing by the effective passband.

Inherent Sun Properties

The broad band values of sun irradiance out-of-the-atmosphere at mean solar distance ${}_s\bar{e}(\infty)$ are obtained from the spectral values of Johnson (1954) ${}_s\bar{e}(\infty,\lambda)$ by

$${}_s\bar{e}(\infty) = \sum_{400}^{1100} {}_s\bar{e}(\infty,\lambda) \ \overline{S_\lambda T_\lambda} \ \Delta\lambda \ / \ \delta\lambda \ . \qquad (A.3)$$

The spectral average inherent sun radiance ${}_s\bar{L}_o(\lambda)$ was computed from

$${}_s\bar{L}_o(\lambda) = {}_s\bar{e}(\infty,\lambda) \ / \ \Omega_s \ , \qquad (A.4)$$

using the mean angular subtense Ω_s of 6.819E-5 steradians based on a mean solar distance of 1.495E8 kilometers and a mean solar diameter of 1.393E6 kilometers. The spectral center sun radiances ${}_sL_o(\lambda)$ were computed using the spectral limb darkening factor $D(\lambda)$ based on the limb darkening functions of Minnaert (1953)

$${}_sL_o(\lambda) = {}_s\bar{L}_o(\lambda) \ / \ D(\lambda) \ . \qquad (A.5)$$

Equations similar to Eq. (A.3) were then used to obtain the broad band inherent sun radiances from the spectral values.

Rayleigh Atmosphere Properties

The spectral values of the Rayleigh total volume scattering coefficient ${}_Rs$ for sea level, 15 degrees Celsius are computed from (Eq. 14 from Penndorf (1957)),

$${}_Rs(\lambda) = 8\pi^3(n^2-1)^2 \ (6+3\rho_n) \ / \ [\ 3\lambda^4\eta(6-7\rho_n)] \ . (A.6)$$

The number density η at atmospheric temperature 15 degrees Celsius is 2.54743E19 cm^{-3} and the depolarization factor ρ_n is 0.035. The refractive index n can be expressed as N' where

$$N' = n-1 \ . \qquad (A.7)$$

Now rewriting Eq. (A.6) in terms of N' and with wavelength in nanometers

$${}_Rs(\lambda) = 3.443E12 \ nm^4 \ m^{-1} \ (N'^2+2N')^2 \ / \ \lambda^4 \ . \quad (A.8)$$

The refractive term N' can be expressed as a function of the refractive modulus $N(0)$ as

APPENDIX A

Table.A.1. Relative spectral response of standards for AVIZ filters.

Wavelength (nm)	FILTER NUMBERS AND MEAN WAVELENGTH					
	No. 2 Blue 478 (nm)	No. 3 Red 664 (nm)	No. 4 Pseudo-Photopic 557 (nm)	No. 5 NIR 765 (nm)	No. 6 S-20 532 (nm)	No. 9 True Photopic 560 (nm)
400	.	.	.	.	0.0000	0.0004
405	.	.	.	.	0.0129	0.0006
410	.	.	.	.	0.0258	0.0012
415	.	.	.	.	0.2969	0.0022
420	.	.	.	.	0.5680	0.0040
425	.	.	.	.	0.7605	0.0073
430	.	.	.	.	0.9530	0.0116
435	.	.	.	.	0.9765	0.0168
440	.	.	.	.	1.0000	0.0230
445	.	.	.	.	0.9920	0 0298
450	.	.	.	.	0.9840	0.0380
455	0.0000	.	.	.	0.9720	0.0480
460	0.0070	.	.	.	0.9600	0.0600
465	0.1487	.	.	.	0.9510	0.0739
470	0.8481	.	0.0000	.	0.9420	0.0910
475	1.0000	.	0.0172	.	0.9355	0.1126
480	0.9329	.	0.0343	.	0.9290	0 1390
485	0.8304	.	0.0677	.	0.9175	0.1693
490	0.1790	.	0.1010	.	0.9060	0.2080
495	0.0292	.	0.1185	.	0.8920	0.2586
500	0.0000	.	0.1360	.	0.8780	0.3230
505	.	.	0.2635	.	0.8560	0.4073
510	.	.	0.3910	.	0.8340	0.5030
515	.	.	0.5085	.	0.8135	0.6082
520	.	.	0.6260	.	0.7930	0.7100
525	.	.	0.7345	.	0.7715	0.7932
530	.	.	0.8430	.	0.7500	0.8620
535	.	.	0.9065	.	0.7250	0.9149
540	.	.	0.9700	.	0.7000	0.9540
545	.	.	0.9850	.	0.6785	0.9803
550	.	.	1.0000	.	0.6570	0.9950
555	.	.	0.9665	.	0.6385	1.0002
560	.	.	0.9330	.	0.6200	0.9950
565	.	.	0.8685	.	0.6030	0.9786
570	.	.	0.8040	.	0.5860	0.9520
575	.	.	0.7195	.	0.5700	0.9154
580	.	.	0.6350	.	0.5540	0 8700
585	.	.	0.5525	.	0.5385	0.8163
590	.	.	0.4700	.	0.5230	0.7570
595	.	.	0.3950	.	0.5060	0.6949
600	.	.	0.3200	.	0.4890	0.6310
605	.	.	0.2630	.	0.4750	0.5668
610	.	.	0.2060	.	0.4610	0.5030

Wavelength (nm)	FILTER NUMBERS AND MEAN WAVELENGTH					
	No. 2 Blue 478 (nm)	No. 3 Red 664 (nm)	No. 4 Pseudo-Photopic 557 (nm)	No. 5 NIR 765 (nm)	No. 6 S-20 532 (nm)	No. 9 True Photopic 560 (nm)
615	.	.	0.1680	.	0.4500	0.4412
620	.	.	0.1300	.	0.4390	0.3810
625	.	.	0.1055	.	0.4260	0.3210
630	.	0.0000	0.0810	.	0.4130	0.2650
635	.	0.0020	0.0657	.	0.3935	0.2170
640	.	0.0486	0.0504	.	0.3740	0.1750
645	.	0.1798	0.0411	.	0.3545	0.1382
650	.	0.5531	0.0318	.	0.3350	0 1070
655	.	0.9948	0.0268	.	0.3190	0.0816
660	.	1.0000	0.0218	.	0.3030	0.0610
665	.	0.9421	0.0188	.	0.2845	0.0446
670	.	0.8625	0.0157	.	0.2660	0.0320
675	.	0.7482	0.0139	.	0.2480	0.0232
680	.	0.4774	0.0120	.	0.2300	0.0170
685	.	0.1585	0.0105	.	0.2105	0.0119
690	.	0.0495	0.0090	.	0.1910	0.0082
695	.	0.0166	0.0080	.	0.1755	0.0057
700	.	0.0000	0.0070	.	0.1600	0.0041
705	.	.	0.0061	.	0.1445	0.0029
710	.	.	0.0053	.	0.1290	0.0021
715	.	.	0.0048	.	0.1170	0.0015
720	.	.	0.0042	0.0000	0.1050	0.0010
725	.	.	0.0038	0.1005	0.0938	0.0007
730	.	.	0.0033	0.2010	0.0826	0.0005
735	.	.	0.0030	0.4155	0.0723	0.0004
740	.	.	0.0026	0.6300	0.0619	0.0003
745	.	.	0.0025	0.8150	0.0558	0.0002
750	.	.	0.0023	1.0000	0.0497	0.0001
755	.	.	0.0020	0.9595	0.0416	0.0001
760	.	.	0.0018	0.9190	0.0335	0.0001
765	.	.	0.0017	0.8495	0.0292	0.0000
770	.	.	0.0016	0.7800	0.0249	.
775	.	.	0.0014	0.6620	0.0206	.
780	.	.	0.0013	0.5440	0.0162	.
785	.	.	0.0012	0.4890	0.0144	.
790	.	.	0.0012	0.4340	0.0125	.
795	.	.	0.0012	0.3720	0.0107	.
800	.	.	0.0011	0.3100	0.0088	.
805	.	.	0.0005	0.2675	0.0075	.
810	.	.	0.0000	0.2250	0.0062	.
815	.	.	.	0.1125	0.0031	.
820	.	.	.	.	.	.

Table A.2. Spectral characteristics summary for AVIZ filters.

Spectral Characteristics				Inherent Sun Properties (Johnson (1954))			Rayleigh Atmosphere Properties (15°C)			Ozone Optical Thickness $a'_{oo}(0)$
Filter Code No.	Peak Wavelength (nm)	Mean Wavelength (nm)	Effective Passband (nm)	Irradiance ($W/m^2\mu m$)	Radiance ($W/\Omega m^2\mu m$) Average	Radiance ($W/\Omega m^2\mu m$) Center	Attenuation Length (m)	Total Scattering Coefficient (per m)	Vertical Radiance Transmittance	
2	475	478	19.9	2.14E+03	3.13E+07	4.07E+07	4.84E+04	2.07E-05	0.839	5.71E-3
3	660	664	30.2	1.57E+03	2.30E+07	2.75E+07	1.86E+05	5.41E-06	0.955	1.81E-3
4	550	557	78.5	1.90E+03	2.78E+07	3.47E+07	8.93E+04	1.15E-05	0.907	3.08E-2
5	750	765	50.4	1.23E+03	1.80E+07	2.10E+07	3.28E+05	3.08E-06	0.974	1.61E-3
6	440	532	183.5	1.91E+03	2.80E+07	3.55E+07	7.22E+04	1.64E-03	0.867	.
9	555	560	106.9	1.89E+03	2.77E+07	3.45E+07	9.22E+04	1.15E-05	0.907	3.07E-2

$$N' = N(0)1E{-}6 . \qquad (A.9)$$

The refractive modulus was computed using the dispersion formula of Edlen (1953) for the refractive modulus $N(0)$ at 15 degrees Celsius at sea level

$$N(0) = 64.328 + 29498.10 / (146 - 1/\lambda^2) + 255.40 / (41 - 1/\lambda^2) , \qquad (A.10)$$

where λ is in μm. The spectral Rayleigh vertical beam transmittance through the atmosphere may be computed by means of the scale height H

$${}_R T_\infty(\lambda) = \exp[-{}_R s(\lambda) H] . \qquad (A.11)$$

The scale height for the *U. S. Standard Atmosphere* (1976) which has a sea level temperature of 15 degrees Celsius, is 8434.7 meters.

Attenuation Length. The attenuation length $\mathfrak{L}$ is defined as that distance at which the signal is attenuated to $1/e$. So monochromatically, the Rayleigh attenuation length is

$${}_R\mathfrak{L}(\lambda) = 1 / {}_R s(\lambda) . \qquad (A.12)$$

A broad band attenuation length is similarly defined as the distance at which the signal is attenuated to $1/e$. Thus

$$\exp(-1) = \exp(-r/{}_R\mathfrak{L}) = \sum_{400}^{1100} \exp[-r\,{}_R s(\lambda)] \overline{S_\lambda T_\lambda}\, \Delta\lambda / \delta\lambda . \qquad (A.13)$$

Equation (A.13) cannot be solved directly for the Rayleigh attenuation length ${}_R\mathfrak{L}$ since the range r is both unknown and in the defining term. However, it can be solved by iteration within acceptable limits.

Volume Scattering Coefficient. The Rayleigh volume scattering coefficient was needed as a lower limit for comparison to the values measured by the integrating nephelometer. Therefore, the limiting value ${}_R s$ is defined as

$${}_R s = \sum_{400}^{1100} {}_R s(\lambda) M(\lambda, 5500K) \overline{S_\lambda T_\lambda}\, \Delta\lambda \Big/ \sum_{400}^{1100} M(\lambda, 5500K) \overline{S_\lambda T_\lambda}\, \Delta\lambda . \qquad (A.14)$$

A Xenon source is used in the nephelometer, therefore the radiant exitance (emittance) in Eq. (A.14) was approximated by a blackbody radiator of 5500 degrees Kelvin $M(\lambda, 5500°K)$. The radiant exitance $M(\lambda, T)$ is

$$M(\lambda, T) = \pi L(\lambda, T) . \qquad (A.15)$$

The $L(\lambda, T)$ is computed from the classical equation (Wolfe (1978) Table 1.7)

$$L(\lambda, T) = c_1 / [\pi\lambda^5 (e^{-x} - 1)] , \qquad (A.16)$$

where

$$c_1 = 2\pi hc^2 = 3.741382E{-}16\ Wm^2 \qquad (A.17)$$

and

$$x = c_2 / (\lambda T) . \qquad (A.18)$$

The c is the speed of light, h is the Planck constant and

$$c_2 = ch / k = 1.438786E{-}2\ mK \qquad (A.19)$$

where k is the Boltzmann constant. The constants are from Driscoll and Vaughn (1978) Table A.1.

Transmittance. The Rayleigh transmittance through the atmosphere was needed as a limit for comparison to the transmittance measurements made with a solar transmissometer. Therefore the broad band Rayleigh transmittance was defined as,

$${}_R T_\infty(0,0) = \sum_{400}^{1100} {}_s L_o(\lambda)\, {}_R T_\infty(\lambda) \overline{S_\lambda T_\lambda}\, \Delta\lambda \Big/ \sum_{400}^{1100} {}_s L_o(\lambda) \overline{S_\lambda T_\lambda}\, \Delta\lambda . \qquad (A.20)$$

where ${}_s L_o(\lambda)$ is the spectral inherent center sun radiance as defined by Eq. (A.5).

Ozone Absorption

The spectral values of ozone absorption a per cm for the Chappuis bands are taken from the tabular values of Vigroux (1953) which are in good agreement with the Inn and Tanaka (1953) values. Since the ozone absorption was to be used in conjunction with the solar transmissometer values, the absorption a per cm for each filter was computed from the spectral values by

$$a = \sum_{400}^{1100} {}_s a(\infty, \lambda) \overline{S_\lambda T_\lambda}\, a_\lambda\, \Delta\lambda \Big/ \sum_{400}^{1100} {}_s a(\infty, \lambda) \overline{S_\lambda T_\lambda}\, \Delta\lambda . \qquad (A.21)$$

The total ozone was from the *U. S. Standard Atmosphere* (1976) which was 0.345 $atm{-}cm$. The ozone optical thickness was computed for each filter from

$$T_\infty(0,0) = \exp[-a\, l_\infty(0)] . \qquad (A.22)$$

APPENDIX A

Rooftop Filters

The relative spectral response values for the broad band sensors used on the rooftop of the Visibility Laboratory building during 1964 are graphed in Fig. A-2 and given in tabular form in Table A.3. The multiplier phototubes had an S-11 spectral response. A summary of the response characteristics of the Rooftop 1964 filters is given in Table A.4.

Rooftop Filter 3 is the photopic sensor. The phototubes were carefully filtered so that they closely approximated the photopic sensor.

Table A.3. Relative spectral response of standards for rooftop 1964 filters.

Wavelength (nm)	FILTER NUMBERS AND MEAN WAVELENGTH			
	No. 1 459 (nm)	No. 2 505 (nm)	No. 3 560 (nm)	NO. 4 661 (nm)
360	.	0.0000	.	.
365	.	0.0366	.	.
370	.	0.0732	.	.
375	.	0.1151	.	.
380	.	0.1570	.	.
385	.	0.1550	.	.
390	.	0.1530	.	.
395	.	0.1810	0.0000	.
400	.	0.2091	0.0004	.
405	.	0.2590	0.0006	.
410	0.0000	0.3090	0.0012	.
415	0.0740	0.3590	0.0022	.
420	0.1480	0.4090	0.0040	.
425	0.3860	0.4685	0.0073	.
430	0.6240	0.5280	0.0116	.
435	0.7635	0.5855	0.0168	.
440	0.9030	0.6430	0.0230	.
445	0.9515	0.6910	0.0298	.
450	1.0000	0.7390	0.0380	.
455	0.9770	0.7765	0.0480	.
460	0.9540	0.8140	0.0600	.
465	0.8875	0.8515	0.0739	.
470	0.8210	0.8890	0.0910	.
475	0.7145	0.9155	0.1126	.
480	0.6080	0.9420	0.1390	.
485	0.5010	0.9630	0.1693	.
490	0.3940	0.9840	0.2080	.
495	0.3020	0.9920	0.2585	.
500	0.2100	1.0000	0.3229	.
505	0.1481	0.9955	0.4072	.
510	0.0861	0.9910	0.5029	.
515	0.0585	0.9605	0.6081	.
520	0.0309	0.9300	0.7099	.
525	0.0198	0.9040	0.7930	.
530	0.0087	0.8780	0.8618	.
535	0.0071	0.8455	0.9147	.
540	0.0054	0.8130	0.9538	.
545	0.0051	0.7740	0.9801	.
550	0.0048	0.7350	0 9948	.
555	0.0044	0.6745	1.0000	.
560	0.0040	0.6140	0.9948	.
565	0.0037	0.5630	0.9784	.
570	0.0034	0.5120	0.9518	.
575	0.0032	0.4900	0.9152	.
580	0.0031	0.4680	0.8698	.
585	0.0029	0.4405	0.8161	.
590	0.0027	0.4130	0.7568	.
595	0.0000	0.3820	0.6948	.
600	.	0.3110	0.6309	0.0000
605	.	0.2540	0.5667	0.0880
610	.	0.1970	0.5029	0.1760
615	.	0.1590	0.4411	0.5020
620	.	0.1210	0.3809	0.8280
625	.	0.1001	0.3209	0.9140
630	.	0.0791	0.2649	1.0000
635	.	0.0684	0.2170	0.9480
640	.	0.0576	0.1750	0.8960
645	.	0.0498	0.1382	0.7975
650	.	0.0420	0.1070	0.6990
655	.	0.0354	0.0816	0.5970
660	.	0.0288	0.0610	0.4950
665	.	0.0240	0.0446	0.4165
670	.	0.0193	0.0320	0.3380
675	.	0.0165	0.0232	0.2890
680	.	0.0137	0.0170	0.2400
685	.	0.0124	0.0119	0.2185
690	.	0.0111	0.0082	0.1970
695	.	0.0111	0.0057	0.1925
700	.	0.0110	0.0041	0.1880
705	.	0.0141	0.0029	0.2300
710	.	0.0173	0 0021	0.2720
715	.	0.0158	0.0015	0.2335
720	.	0.0142	0.0010	0.1990
725	.	0.0144	0.0007	0.1895
730	.	0.0146	0.0005	0.1800
735	.	0.0141	0.0004	0.1630
740	.	0.0135	0.0003	0.1460
745	.	0.0122	0.0002	0.1265
750	.	0.0109	0.0001	0.1070
755	.	0.0096	0.0001	0.0912
760	.	0.0082	0.0001	0.0754
765	.	0.0068	0 0000	0.0628
770	.	0.0055	.	0.0501
775	.	0.0046	.	0.0405
780	.	0.0036	.	0.0310
785	.	0.0028	.	0.0239
790	.	0.0020	.	0.0167
795	.	0.0015	.	0.0127
800	.	0.0011	.	0.0086

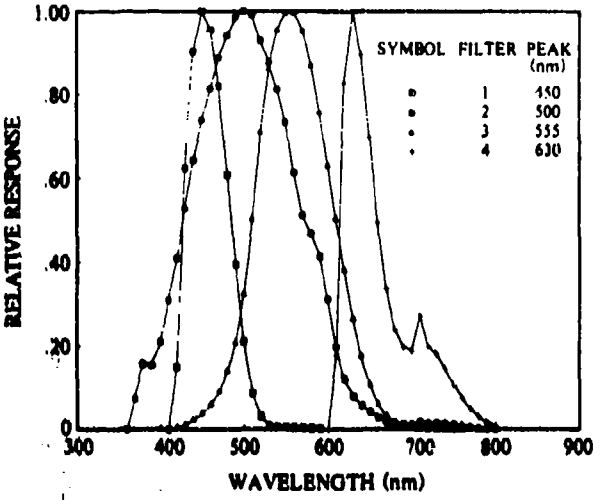

Fig. A-2. Standard spectral responses for Visibility Laboratory rooftop filters.

Table A.4. Spectral characteristics summary for rooftop 1964 filters.

Spectral Characteristics				Inherent Sun Properties [Johnson (1954)]			Rayleigh Atmosphere Properties (15°C)			Ozone Optical Thickness $d'_{oo}(0)$
Filter Code No.	Peak Wavelength (nm)	Mean Wavelength (nm)	Effective Passband (nm)	Irradiance ($W/m^2\mu m$)	Radiance ($W/\Omega\, m^2\mu m$) Average	Radiance ($W/\Omega\, m^2\mu m$) Center	Attenuation Length (m)	Total Scattering Coefficient (per m)	Vertical Radiance Transmittance	
1	450	459	58.1	2.08E+03	3.04E+07	4.00E+07	4.11E+04	2.47E-05	0.812	3.70E-3
2	500	505	151.9	1.95E+03	2.86E+07	3.66E+07	5.94E+05	1.87E-05	0.852	1.60E-2
3	555	560	106.8	1.89E+03	2.77E+07	3.45E+07	9.22E+04	1.15E-05	0.907	3.07E-2
4	630	661	61.4	1.59E+03	2.33E+07	2.79E+07	1.80E+05	5.78E-06	0.952	2.20E-2

APPENDIX B

GLOSSARY AND NOTATION

The notation used in reports and journal articles produced by the Visibility Laboratory staff follows, in general, the rules set forth in pages 499 and 500, Duntley *et al.* (1957). These rules are:

- Each optical property is indicated by a basic (parent) symbol.
- A presubscript may be used with the parent symbol as an identifier, *e.g.*, b indicates background while t denotes an object, *i.e.* target.
- A postsubscript may be used to indicate the length of a path of sight, *e.g.*, r denotes an apparent property as measured at the end of a path of sight of length r, while o denotes an inherent property based on the hypothetical concept of a photometer located at zero distance from an object, *i.e.* target.
- A postsuperscript* or postsubscript$_*$, is employed as a mnemonic symbol signifying that the radiometric quantity has been generated within the path or path segment by the scattering of ambient light reaching the path from all directions and/or by emission.
- The parenthetical attachments to the parent symbol denote altitude and direction. The letter z indicates altitude in general; z_t is used to specify the altitude of a target. The direction of a path of sight is specified by the zenith angle θ and the azimuth ϕ. In the case of irradiances, the downwelling irradiance is designated by d, the upwelling by u.
- The radiometric symbols used herein now correspond to the OSA recommendations in Section 1 of Driscoll and Vaughn (1978). Prior to June 1980, the symbol used for radiance L was N, for irradiance E was H, and for attenuation length $\mathfrak{L}$ was L.

Symbol	Units	Quantity
$A(z)$	none	Albedo at altitude z, defined $A(z) = E(z,u) / E(z,d)$.
$a(z)$	m^{-1}	Absorption coefficient.
$C(z)$	$sr^{-1}\,m^{-1}$	Diffuse component of the solar almucantar sky radiance ratio to the sun scalar irradiance and relative airmass $C(z) = \int_{2\pi} L(z,\theta',\phi')\sigma(z,\beta')d\Omega \;/\; {}_s\epsilon(z) + L_{s_o}(z) \;/\; {}_s\epsilon(z)$.
c	m/s	Speed of light $c = 2.99792458E8$.
c_1	Wm^2	First radiation constant $c_1 = 2\pi hc^2 = 3.741832E{-}16$.
c_2	mK	Second radiation constant $c_2 = ch/k = 1.438786E{-}2$.
$D(z)$	none	Radiance distribution function $D(z) = \int_{2\pi} L(z,\theta',\phi')sec\theta' d\Omega \;/\; \epsilon(z)$.
$D(\lambda)$	none	Limb darkening factor relating the average sun radiance and the center sun radiance $D(\lambda) = {}_s\bar{L}_o \;/\; {}_sL_o$.
E_λ	W/m^2	Spectral irradiance (formerly symbol H) defined as $E_\lambda = \int_{2\pi} L_\lambda(z,\theta,\phi)\cos\theta\, d\Omega$.

Symbol	Units	Quantity
E	$W/m^2\,\mu m$	Broad band sensor irradiance, defined as $E = \int_0^\infty E_\lambda \overline{S_\lambda T_\lambda}\, d\lambda \,/\, \delta\lambda$.
$E(z,d)$	W/m^2	Irradiance produced by downwelling flux as determined on a horizontal flat plate at altitude z [formerly $H(z,d)$]. In this report d is used in place of the minus sign in the notation [$H(z,-)$] which appears in Duntley (1969). This property may be defined by the equation $E(z,d) = \int_{2\pi} L(z,\theta',\phi') \cos\theta' \, d\Omega'$.
$E(z,u)$	W/m^2	Irradiance produced by the upwelling flux as determined on a horizontal flat plane at altitude z [formerly $H(z,u)$]. Here u is substituted for the plus sign formerly used in the notation [$H(z,+)$].
$H(z)$	m	Scale height at altitude z, the height of a homogeneous atmosphere having the density of the layer at altitude z.
h	J/s	Planck constant $h = 6.626176E{-}34$.
k	J/K	Boltzmann constant $k = 1.380662E{-}23$.
L_λ	$W/sr\ m^2$	Spectral radiance (former symbol N).
L	$W/sr\ m^2\,\mu m$	Broad band sensor radiance is defined as $L = \int_0^\infty L_\lambda \overline{S_\lambda T_\lambda}\, d\lambda \,/\, \delta\lambda$.
$L_0(z_t,\theta,\phi)$	$W/sr\ m^2$	Inherent radiance based on the hypothetical concept of a photometer located at zero distance from an object at altitude z in the direction specified by zenith angle θ and azimuth ϕ.
$L_r(z,\theta,\phi)$	$W/sr\ m^2$	Apparent radiance as determined at altitude z, from the end of a path of sight of length r at zenith angle θ and azimuth ϕ. This property may be defined by $L_r(z,\theta,\phi) = L_0(z_t,\theta,\phi)\,T_r(z,\theta) + L_r^*(z,\theta,\phi)$.
$L(\lambda,T)$	$W/sr\ m^2$	Black body radiance at wavelength λ and temperature T.
$L_q(z,\theta,\phi)$	$W/sr\ m^2$	Equilibrium radiance at altitude z with the direction of the path of sight specified by zenith angle θ and azimuth ϕ. This property is a point function of position and direction. As discussed by Duntley *et al.* (1957), many image transmission phenomena are most clearly understood in terms of the concept of equilibrium radiance. This concept is a natural consequence of the equation of transfer which states analytically that in any path segment the difference between the output and input radiances is attributable to a gain term and a loss term, such that some unique equilibrium radiance $L_q(z,\theta,\phi)$ must exist at each point such that the loss of radiance within the path segment is exactly balanced by the gain, *i.e.*, $\Delta L(z,\theta,\phi) = 0$.

APPENDIX B

Symbol	Units	Quantity
		By virtue of this concept and the equation of transfer, one can show that each segment of every path of sight has associated with it an equilibrium radiance, and that the space rate of change in image forming radiance caused by the path segment is in such a direction as to cause the output radiance to be closer to the equilibrium radiance than is the input radiance. This segment by segment convergence of the apparent radiance of the object field to the dynamic equilibrium radiance was clearly illustrated by the data in the 1957 paper referenced above.
$L_e(z,\theta,\phi)$	$W/sr\ m^2$	Path function at altitude z with the direction of the path of sight specified by zenith angle θ and azimuth ϕ. This property is defined by the equation $L_e(z,\theta,\phi) = L_{e_s}(z,\theta,\phi) + L_{e_a}(z)$.
$L_{e_s}(z,\theta,\phi)$	$W/sr\ m^2$	Path function due to scattering, defined by $L_e(z,\theta,\phi) = \int_{4\pi} \sigma(z,\beta')L(z,\theta',\phi')\,d\Omega'$.
$L_{e_a}(z)$	$W/sr\ m^2$	Path function due to emittance (absorption) $L_{e_a}(z) = a(z)\,L(\lambda,T)$.
$L_r^*(z,\theta,\phi)$	$W/sr\ m^2$	Path radiance as determined at altitude z at the end of a path of sight of length r in the direction of zenith angle θ and azimuth ϕ.
$L_\infty^*(z,\theta,\phi)$	$W/sr\ m^2$	Sky radiance at altitude z, zenith angle θ and azimuth ϕ. Also the path radiance for the path of sight of length ∞ from out of the atmosphere to altitude z.
${}_sL_\infty(z,\theta_s,\phi)$	$W/sr\ m^2$	Apparent radiance of the center of the solar disk as determined from the end of a path of sight of length ∞ from out of the atmosphere to altitude z at the zenith angle of the sun θ_s.
$\mathfrak{L}(z)$	m	Attenuation length at altitude z. The attenuation length is the distance at which the signal is attenuated to 1/e.
$M(\lambda,T)$	W/m^2	Black body exitance (emittance) $M(\lambda,T) = \pi L(\lambda,T)$.
$m(\lambda,T)$	W/m^2	Black body scalar exitance (emittance) $m(\lambda,T) = 4\pi L(\lambda,T)$.
$m_e(z)$	W/m^3	Scalar exitance (emittance) per length $m_e(z) = \int_{4\pi} L_e(z,\theta,\phi)\,d\Omega$.
$m_{e_s}(z)$	W/m^3	Scalar exitance (emittance) per length due to scattering $m_{e_s}(z) = \int_{4\pi} L_{e_s}(z,\theta,\phi)\,d\Omega = \epsilon(z)s(z)$.
$m_{e_a}(z)$	W/m^3	Scalar exitance (emittance) per length due to absorption $m_{e_a}(z) = a(z)m(\lambda,T)$.
$m_m(z,\theta)$	kg/m^2	Absolute air mass at angle θ $m_m(z,\theta) = \int_z^\infty \rho(z)\,dr$.

Symbol	Units	Quantity
$m_m(z,\theta)/m_m(z,0°)$	none	Relative optical air mass.
$m(\theta_s)$	none	Relative optical airmass at zenith angle of the sun, shorthand for $m_m(z,\theta_s)/m_m(z,0°)$.
$N(z)$	none	Refractive modulus $N(z) = [n(z) - 1]E6$.
$n(z)$	none	Refractive index.
$Q(z)$	none	Optical scattering mixing ratio at altitude z. This quantity is defined as the ratio of the total volume scattering coefficient at altitude z, to the molecular (or Rayleigh) volume scattering coefficient at the same altitude z. $Q(z) = s(z)/_R s(z)$.
$\mathcal{Q}(z,\beta)$	none	Volume scattering function ratio at altitude z. This quantity is defined as the ratio of the total volume scattering function at altitude z and scattering angle β, to the molecular (or Rayleigh) volume scattering function at the same altitude and scattering angle. $\mathcal{Q}(z,\beta) = \sigma(z,\beta) / {}_R\sigma(z,\beta)$.
r	m	Path length, for paths of sight at zenith angles 0 to 70 degrees, $r = \sec\theta\ \Delta z$.
$\overline{S_\lambda T_\lambda}$	none	Standardized relative spectral response of filter/cathode combination where S_λ is spectral sensitivity of the multiplier phototube cathode and T_λ is spectral transmittance of optical filter. The relative spectral response values are normalized to the peak value.
$s(z)$	m^{-1}	Total volume scattering coefficient as determined at altitude z. This property may be defined by the equations $$s(z) = \int_{4\pi}\sigma(z,\beta)\,d\Omega = {}_R s(z) + {}_M s(z).$$ In the absence of atmospheric absorption, the total volume scattering coefficient is numerically equal to the attenuation coefficient.
${}_M s(z)$	m^{-1}	Volume scattering coefficient for Mie *i.e.* particulate or droplet, scattering at altitude z.
${}_R s(z)$	m^{-1}	Volume scattering coefficient for Rayleigh *i.e.* molecular, scattering at altitude z.
T	K	Absolute temperature in degrees Kelvin.
$T_r(z,\theta)$	none	Radiance transmittance as determined at altitude z for a path of sight of length r at zenith angle θ (formerly referred to as "beam" transmittance). This property is independent of azimuth in atmospheres having horizontal uniformity. It is always the same for the designated path of sight or its reciprocal.
$T_m(z,\theta)$	none	Radiance transmitance for the path of sight at zenith angle θ from out of the atmosphere to the altitude z.

APPENDIX B

Symbol	Units	Quantity
$t_{\Delta z}(z)$	none	Optical thickness $t_{\Delta z}(z) = \int_{z_1}^{z} \alpha(z)\,dz$.
${}_a t_{\Delta z}(z)$	none	Absorption optical thickness ${}_a t_{\Delta z}(z) = \int_{z_1}^{z} a(z)\,dz$.
${}_M t_{\Delta z}(z)$	none	Mie optical thickness ${}_M t_{\Delta z}(z) = \int_{z_1}^{z} {}_M s(z)\,dz$.
${}_R t_{\Delta z}(z)$	none	Rayleigh or molecular optical thickness ${}_R t_{\Delta z}(z) = \int_{z_1}^{z} {}_R s(z)\,dz$.
w	J/m^3	Radiant density.
W	W	Watt W = J/s.
z	m	Altitude, usually used as above ground level.
z_t	m	Altitude of any applicable object or target.
$\alpha(z)$	m^{-1}	Volume attenuation coefficient as determined at altitude z. $\alpha(z) = a(z) + s(z)$.
β	deg	Symbol for scattering angle of flux from a light source. It is equal to the angle between the line from the source to any unit scattering volume and the path of a ray scattered off this direct line. See illustration.
Δ	none	Symbol to indicate incremental quantity and used with r and z to indicate small, discrete increments in path length r and altitude z.
$\delta\lambda$	nm	Effective passband (formerly designated "response area") for a filtered sensor is defined as $\delta\lambda = \int_{0}^{\infty} \overline{S_\lambda T_\lambda}\,d\lambda$.

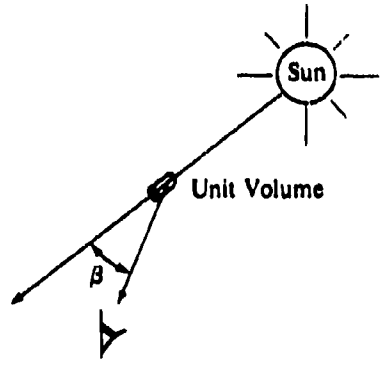

Symbol	Units	Quantity
$\epsilon(z)$	W/m^2	Scalar irradiance. This may be defined as the radiant flux arriving at a point, from all directions about that point, at altitude z (Tyler and Preisendorfer (1962)). $\epsilon(z) = \int_{4\pi} L(z,\theta',\phi')\,d\Omega'$.
${}_d\epsilon(z)$	W/m^2	Diffuse scalar irradiance ${}_d\epsilon(z) = \epsilon(z) - {}_s\epsilon(z)$.
${}_s\epsilon(z)$	W/m^2	Sun scalar irradiance at altitude z ${}_s\epsilon(z) = {}_s\epsilon(\infty)\,T_m(z,\theta_s)$.
ζ	m	Radius of the earth.
θ	deg	Symbol for zenith angle. This symbol is usually used as one of two coordinates to specify the direction of a path of sight.
θ'	deg	Symbol for zenith angle usually used as one of two coordinates to specify the direction of a discrete portion of the sky.
θ_s	deg	Zenith angle of the sun.
λ	nm	Symbol for wavelength.
$\bar{\lambda}$	nm	Mean wavelength is defined as $\bar{\lambda} = \int_0^\infty \lambda \overline{S_\lambda T_\lambda}\,d\lambda \,/\, \delta\lambda$.
$\mu(z,\beta)$	sr^{-1}	Ratio of solar almucantar sky radiance to scalar sun irradiance and airmass. $\mu(z,\beta) = L^\circ_m(z,\theta_s,\beta) \,/\, [{}_s\epsilon(z)m(\theta_s)]$.
$\xi(z)$	W/m^2	Net irradiance. $\xi(z) = E(z,d) - E(z,u)$.
$\rho(z)$	kg/m^3	Density at altitude z.
$\sigma(z,\beta)$	$m^{-1}sr^{-1}$	Symbol for volume scattering function. Parenthetical symbols are z to designate altitude and β to designate the scattering angle from a source.
$\sigma(z,\beta)/s(z)$	sr^{-1}	Normalized volume scattering function. This may be defined by the equation $\int_{4\pi} [\sigma(z,\beta) \,/\, s(z)]\,d\Omega = 1$.
$\tau_{\Delta z}(z,\beta)$	sr	Optical thickness function. $\tau_{\Delta z}(z,\beta) = \int_{z_1}^{z_2} \sigma(z,\beta)\,dz$.

APPENDIX B

Symbol	Units	Quantity
ϕ	deg	Symbol for azimuth. The azimuth is the angle in the horizontal plane of the observer between a fixed point and the path of sight. The fixed point may be for example, true North, the bearing of the sun, or the bearing of the moon. This symbol is usually used as one of two coordinates to specify the direction of a path of sight.
ϕ'	deg	This symbol for azimuth is usually used as one of two coordinates to specify the direction of a discrete portion of the sky.
ψ	deg	Angular solar radius at true earth-to-sun distance.
$\bar{\psi}$	deg	Angular solar radius at mean solar distance.
Ω	*sr*	Symbol for solid angle. For a hemisphere, $\Omega = 2\pi$ steradians. For a sphere, $\Omega = 4\pi$ steradians.
$\omega(z)$	none	Single scattering albedo $\omega(z) = s(z) / \alpha(z)$.

Table B.1. Notational equivalencies.

Chandrasekhar (1960)		Visibility Laboratory	
Symbol	Definition	Symbol	Definition
E	Radiant energy	E	Irradiance
πF	Net flux	ξ	Net irradiance
I	Specific intensity	$L(z,\theta,\phi)$	Radiance
J	Average intensity	$\epsilon/4\pi$	Average radiance
j	Mass emission coefficient	$\frac{L_*(z,\theta,\phi)}{\rho(z)}$	Path function/density
$j\rho$	Mass emission coefficient × density	$L_*(z,\theta,\phi)$	Path function
$j^{(s)}$	Mass emission coefficient due to scattering	$\frac{L_{*_s}(z,\theta,\phi)}{\rho(z)}$	Path function due to scattering divided by the density
k	Mass absorption coefficient	α/ρ	Attenuation coefficient divided by the density
$k\rho$	Mass absorption coefficient × density	$\alpha(z)$	Attenuation coefficient
$p(\cos\Theta)$	Phase function	$4\pi\sigma(\beta)/\alpha$	Four π times volume scattering function/attenuation coefficient
s	Thickness	r	Path length
$\mathfrak{J}$	Source function	L_q	Equilibrium radiance
u	Integrated energy density	w	Radiant density
ω_0	Single scattering albedo	$\omega(z)$	Single scattering albedo
Θ	Scattering angle	β	Scattering angle
ϑ	Polar angle	θ	Zenith angle
μ	cosine of polar angle	$\cos\theta$	cosine of zenith angle
ν	Frequency	$1/\lambda$	Inverse wavelength
ρ	Density	ρ	Density
τ	Normal optical thickness	$t_{\Delta z}$	Optical thickness
φ	Azimuth	ϕ	Azimuth
ω	Solid angle	Ω	Solid angle

APPENDIX C

VISIBILITY LABORATORY CONTRACTS AND RELATED PUBLICATIONS

Previous Related Contracts:
F19628-73-C-0013, F19628-76-C-0004

PUBLICATIONS:

Duntley, S.Q., R.W. Johnson, J.I. Gordon, and A. R. Boileau, "Airborne Measurements of Optical Atmospheric Properties at Night", University of California, San Diego, Scripps Institution of Oceanography, Visibility Laboratory, SIO Ref. 70-7, AFCRL-70-0137, NTIS No. AD 870 734 (1970).

Duntley, S.Q., R.W. Johnson, and J.I. Gordon, "Airborne Measurements of Optical Atmospheric Properties in Southern Germany", University of California, San Diego, Scripps Institution of Oceanography, Visibility Laboratory, SIO Ref. 72-64, AFCRL-72-0255, NTIS No AD 747 490 (1972a).

Duntley, S.Q., R.W. Johnson, and J.I. Gordon, "Airborne and Ground-Based Measurements of Optical Atmospheric Properties in Central New Mexico", University of California, San Diego, Scripps Institution of Oceanography, Visibility Laboratory, SIO Ref. 72-71, AFCRL-72-0461, NTIS No. AD 751 936 (1972b).

Duntley, S.Q., R.W. Johnson, and J.I. Gordon, "Airborne Measurements of Optical Atmospheric Properties, Summary and Review", University of California, San Diego, Scripps Institution of Oceanography, Visibility Laboratory, SIO Ref. 72-82, AFCRL-72-0593, NTIS No. AD 754 898 (1972c).

Duntley, S.Q., R.W. Johnson, and J.I. Gordon, "Airborne Measurements of Optical Atmospheric Properties in Southern Illinois", University of California, San Diego, Scripps Institution of Oceanography, Visibility Laboratory, SIO Ref. 73-24, AFCRL-TR-73-0422, NTIS No. AD 774 597 (1973).

Duntley, S.Q., R.W. Johnson, and J.I. Gordon, "Airborne and Ground-Based Measurements of Optical Atmospheric Properties in Southern Illinois", University of California, San Diego, Scripps Institution of Oceanography, Visibility Laboratory, SIO Ref. 74-25, AFCRL-TR-74-0298, NTIS No. ADA 013 164 (1974).

Duntley, S.Q., R.W. Johnson, and J.I. Gordon, "Airborne Measurements of Optical Atmospheric Properties in Western Washington", University of California, San Diego, Scripps Institution of Oceanography, Visibility Laboratory, SIO Ref. 75-24, AFCRL-TR-75-0414, NTIS No. ADA 026 036 (1975a).

Duntley, S.Q., R.W. Johnson, and J.I. Gordon, "Airborne Measurements of Optical Atmospheric Properties, Summary and Review II", University of California, San Diego, Scripps Institution of Oceanography, Visibility Laboratory, SIO Ref. 75-26, AFCRL-TR-75-0457, NTIS No. ADA 022 675 (1975b).

Duntley, S.Q., R.W. Johnson, and J.I. Gordon, "Airborne Measurements of Optical Atmospheric Properties in Northern Germany", University of California, San Diego, Scripps Institution of Oceanography, Visibility Laboratory, SIO Ref. 76-17, AFGL-TR-76-0188, NTIS No. ADA 035 571 (1976).

Duntley, S.Q., R.W. Johnson, and J.I. Gordon, "Airborne Measurements of Atmospheric Volume Scattering Coefficients in Northern Europe, Spring 1976", University of California, San Diego, Scripps Institution of Oceanography, Visibility Laboratory, SIO Ref. 77-8, AFGL-TR-77-0078, NTIS No. ADA 046 290 (1977).

Duntley, S.Q., R.W. Johnson, and J.I. Gordon, "Airborne Measurements of Atmospheric Volume Scattering Coefficients in Northern Europe, Fall 1976", University of California, San Diego, Scripps Institution of Oceanography, Visibility Laboratory, SIO Ref. 78-3, AFGL-TR-77-0239, NTIS No. ADA 057 144 (1978a).

Duntley, S.Q., R.W. Johnson, and J.I. Gordon, "Airborne Measurements of Atmospheric Volume Scattering Coefficients in Northern Europe, Summer 1977", University of California, San Diego, Scripps Institution of Oceanography, Visibility Laboratory, SIO Ref. 78-28, AFGL-TR-78-0168, NTIS No. ADA 068 611 (1978b).

Duntley, S.Q., R.W. Johnson, and J.I. Gordon, "Airborne Measurements of Optical Atmospheric Properties, Summary and Review III", University of California, San Diego, Scripps Institution of Oceanography, Visibility Laboratory, SIO Ref. 79-5, AFGL-TR-78-0286, NTIS No. ADA 073 121 (1978c).

Fitch, B.W. and T.S. Cress, "Measurements of Aerosol Size Distribution in the Lower Troposphere over Northern Europe", University of California, San Diego, Scripps Institution of Oceanography, Visibility Laboratory, SIO Ref. 81-18, AFGL-TR-80-0192, NTIS No. ADA 104 272 (1981). Also J.Appl.Met. 20, No. 10, 1119-1128.

Gordon, J.I., "Model for a Clear Atmosphere", J. Opt. Soc. Am. 59, 14-18 (1969).

Gordon, J.I., J. L. Harris, Sr., and S.Q. Duntley, "Measuring Earth-to-Space Contrast Transmittance from Ground Stations", Appl. Opt. 12, 1317-1324 (1973).

Gordon, J.I., C. F. Edgerton, and S.Q. Duntley, "Signal-Light Nomogram", J. Opt. Soc. Am. 65, 111-118 (1975).

Gordon, J.I., "Daytime Visibility, A Conceptual Review", University of California, San Diego, Scripps Institution of Oceanography, Visibility Laboratory, SIO Ref. 80-1, AFGL-TR-79-0257, NTIS No. ADA 085 451 (1979).

Hering, W. S., "An Operational Technique for Estimating Visible Spectrum Contrast Transmittance", University of California, San Diego, Scripps Institution of Oceanography, Visibility Laboratory, SIO Ref. 82-1, AFGL-TR-81-0198 (1981a).

Hering, W.S., "Assessment of Operational Techniques for Estimating Visible Spectrum Contrast Transmit-

tance", *SPIE Proceedings on Atmospheric Effects on System Performance*, Vol. 205, pp. 119-125 (1981b).

Johnson, R.W., and J.I. Gordon, "Airborne Measurements of Atmospheric Volume Scattering Coefficients in Northern Europe, Winter 1978", University of California, San Diego, Scripps Institution of Oceanography, Visibility Laboratory, SIO Ref. 79-25, AFGL-TR-79-0159, NTIS No. ADA 082 044 (1979).

Johnson, R.W., W. S. Hering, J.I. Gordon, B. W. Fitch, and J.S. Shields, "Preliminary Analysis & Modelling Based Upon Project OPAQUE Profile and Surface Data", University of California, San Diego, Scripps Institution of Oceanography, Visibility Laboratory, SIO Ref. 80-5, AFGL-TR-79-0285, NTIS ADB 052 172L (1979).

Johnson, R.W., "Airborne Measurements of European Atmospheric Scattering Coefficients", *SPIE Proceedings on Atmospheric Effects on Radiative Transfer*, 195, 31-38 (1979).

Johnson, R.W. and J.I. Gordon, "Airborne Measurements of Atmospheric Volume Scattering Coefficients in Northern Europe, Summer 1978", University of California, San Diego, Scripps Institution of Oceanography, Visibility Laboratory, SIO Ref. 80-20, AFGL-TR-80-0207, NTIS No. ADA 097 134 (1980).

Johnson, R.W. and W.S. Hering, "Measurements of Optical Atmospheric Quantities in Europe and Their Application to Modelling Visible Spectrum Contrast Transmittance", *AGARD Proceedings on Special Topics in Optical Propagation*, AGARD-CP-300, pp. 14-1 to 14-12 (1981a).

Johnson, R.W. and W. S. Hering, "An Analysis of Natural Variations in Measured European Sky and Terrain Radiances", University of California, San Diego, Scripps Institution of Oceanography, Visibility Laboratory, SIO Ref. 82-6, AFGL-TR-81-0317 (1981b).

Johnson, R.W., "Winter and Summer Measurements of European Very Low Altitude Volume Scattering Coefficients," University of California, San Diego, Scripps Institution of Oceanography, SIO Ref. 81-26, AFGL-TR-81-0154, NTIS No. ADA 106 363 (1981a).

Johnson, R.W., "Spring and Fall Measurements of European Very Low Altitude Volume Scattering Coefficients", University of California, San Diego, Scripps Institution of Oceanography, Visibility Laboratory, SIO Ref. 81-33, AFGL-TR-81-0237, NTIS No. ADA 108 879 (1981b).

Johnson, R.W., "Daytime Visibility and Nephelometer Measurements Related to its Determination", Atmospheric Environment, 15, 10/11, 1835 (1981c).

Johnson, R.W., "Airborne Measurements of European Sky and Terrain Radiances", University of California, San Diego, Scripps Institution of Oceanography, Visibility Laboratory, SIO Ref. 82-2, AFGL-TR-81-0275 (1981d).

Johnson, R.W. and B.W. Fitch, "A Review of Measured Atmospheric Optical Properties and Their Contemporary Aerosol Size Distributions", University of California, San Diego, Scripps Institution of Oceanography, Visibility Laboratory, SIO Ref. 82-22, AFGL-TR-82-0049 (1981).

Johnson, R.W. and J.I. Gordon, "A Review of Optical Data Analysis Related to the Modelling of Visible and Optical Infrared Atmospheric Properties", University of California, San Diego, Scripps Institution of Oceanography, Visibility Laboratory, SIO Ref. 83-5, AFGL-TR-82-0086 (1981).

Shields, J.S., "An Analysis of Infrared and Visible Atmospheric Extinction Coefficient Measurements in Europe", University of California, San Diego, Scripps Institution of Oceanography, Visibility Laboratory, SIO Ref. 82-4, AFGL-TR-81-0251 (1981).